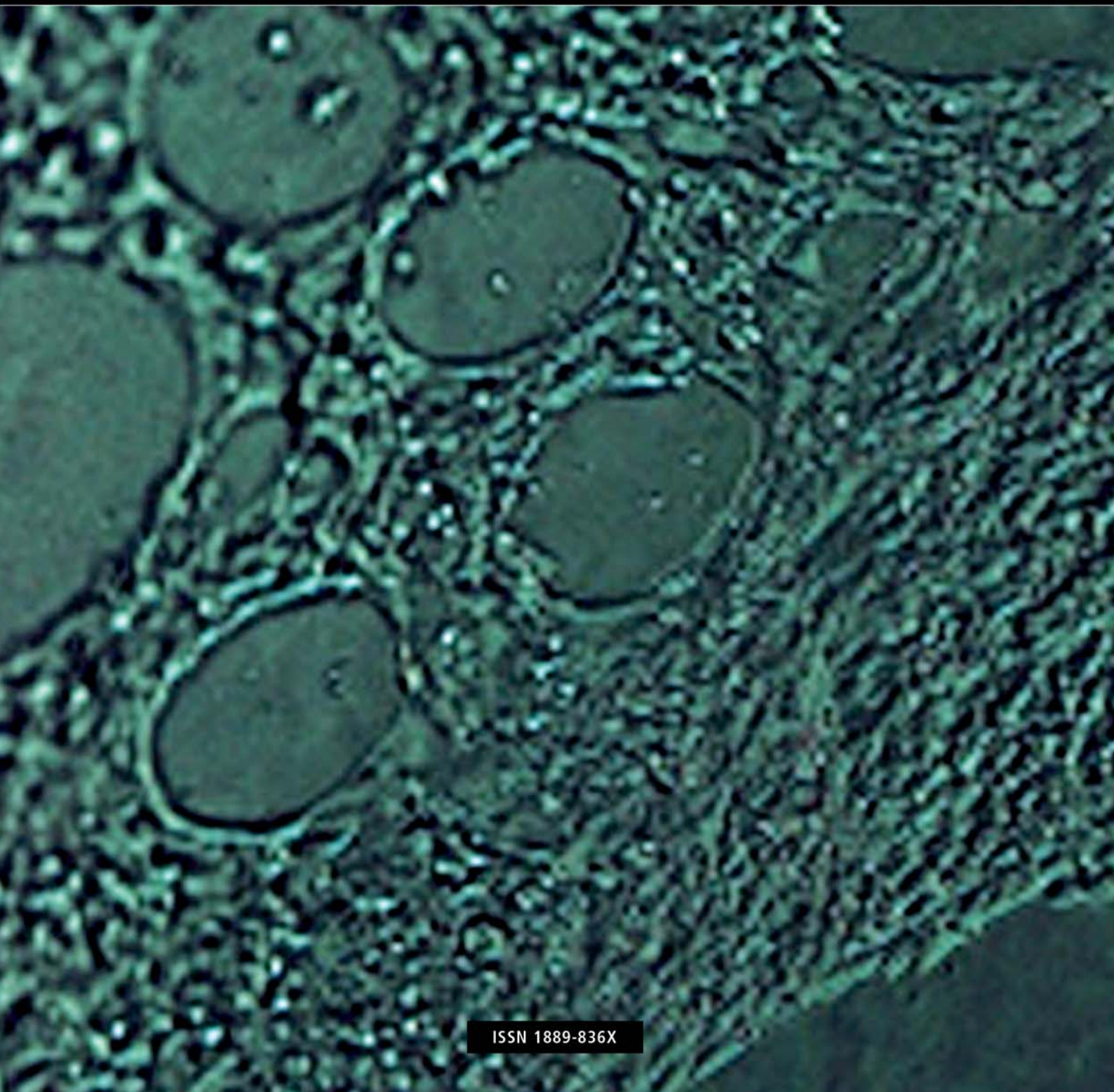
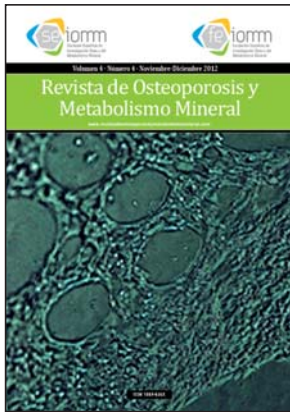


Volume 4 · Number 4 · November-December 2012

# Revista de Osteoporosis y Metabolismo Mineral

[www.revistadeosteoporosisymetabolismomineral.com](http://www.revistadeosteoporosisymetabolismomineral.com)





## Our cover

Angiogenic endothelial cells from the umbilical vein (HUVEC)

### Authors:

Raquel Santiago Mora, Antonio Casado Díaz, y José Manuel Quesada

*Director*

**Manuel Sosa Henríquez**

*Editor Head*

**M<sup>a</sup> Jesús Gómez de Tejada Romero**

**Sociedad Española de Investigación Ósea y del Metabolismo Mineral (SEIOMM)**

*President*

**Javier del Pino Montes**

*Vice-president*

**Josep Blanch Rubio**

*Secretariat*

**M<sup>a</sup> Jesús Moro Álvarez**

*Treasure*

**Carmen Valero Díaz de Lamadrid**

Paseo de la Castellana, 135 (7<sup>a</sup> planta)  
28046 Madrid

Telf: +34-917906834

Fax: +34-917906869

e-mail: [seiomm@seiomm.org](mailto:seiomm@seiomm.org)

<http://www.seiomm.org>

*Edición*



Avda. Reina Victoria, 47 (6<sup>o</sup> D)  
28003 Madrid

Telf./Fax +34-915 538 297

e-mail: [correo@ibanezyplaza.com](mailto:correo@ibanezyplaza.com)

<http://www.ibanezyplaza.com>

*Graphic design*

**Concha García García**

*English translation*

**Andrew Stephens**

*Impresion*

**Imprenta Narcea**

*Valid Support*

**32/09-R-CM**

*Legal Deposit*

**AS-4777-09**

**ISSN 1889-836X**

## SUMMARY Vol. 4 - Nº 4 - November-December 2012

**105**

### EDITORIAL

**Sclerostin and bone in diabetes mellitus type 2**  
Jódar Gimeno E

**109**

### ORIGINALS

**Variables which influence concentrations of sclerostin in patients with diabetes mellitus type 2 and its association with bone metabolism**

García-Martín A, Reyes-García R, Rozas-Moreno P, Varsavsky M, Luque-Fernández I, Avilés-Pérez MD, Muñoz-Torres M

**117**

**Osteogenic effects of PTHrP (107-111) loaded in bioceramics in a model of bone regeneration after a cavitory defect in the femur of a rabbit**

Lozano D, Trejo CG, Manzano M, Doadrio JC, Salinas AJ, Dapía S, Caeiro Rey JR, Gómez-Barrena E, Vallet-Regí M, García-Honduvilla N, Buján J, Esbrit P

**127**

**Osteointegration and biocompatibility *in vivo* of bio-inspired silicon carbide ceramics in an experimental model in rabbits**

Guede D, Pereiro I, Solla E, Serra J, López-Peña M, Muñoz F, González-Cantalapiedra A, Caeiro JR, González P

**133**

**Expression of RANKL and OPG in primary osteoblasts**

Delgado-Calle J, Sañudo C, Sumillera M, Garcés CM, Riancho JA

**141**

### CLINICAL NOTES

**Bone metastases and cord compression debut as follicular thyroid carcinoma**

Civantos Modino S, Navea Aguilera C, Pavón de Paz I, Almodovar Ruiz F, Elviro Peña MR

**145**

**Costal right metastasis of prostate adenocarcinoma**

Espasa Font L, Supervía A, Del Baño F, Sarbu MI

**149**

**Hypercalcemia crisis due to complex parathyroid tumour: a diagnostic and surgical dilemma**

Ovejero Gómez VJ, Díez Muñoz-Alique M, Díez Lizuaín ML, Pérez Martín A, Azcarretazábal González-Ontaneda T, Ingelmo Setien A

Submit originals:

[revistadeosteoporosisymetabolismomineral@ibanezyplaza.com](mailto:revistadeosteoporosisymetabolismomineral@ibanezyplaza.com)

On-line version:

<http://www.revistadeosteoporosisymetabolismomineral.com>

**Editorial Committee****Teresita Bellido, Ph.D.**

Department of Medicine, Division of Endocrinology. Indiana University School of Medicine. Indianapolis, Indiana. Estados Unidos

**Ernesto Canalis, MD, PhD**

St Francis Hospital and Medical Center, Hartford, Connecticut. University of Connecticut. School of Medicine, Farmington, Connecticut. Estados Unidos

**Patricia Clark Peralta, MD, PhD**

Facultad de Medicina, UNAM. Unidad Clínica Epidemiológica. Hospital Infantil Federico Gómez. México DF. México

**Dr. Javier del Pino Montes**

Departamento de Medicina. Universidad de Salamanca. Sección de Reumatología. Hospital Universitario de Salamanca. Salamanca. España

**Dr. Manuel Díaz Curiel**

Universidad Autónoma de Madrid. Unidad de Metabolismo Óseo. Hospital Fundación Jiménez Díaz. Instituto de Investigación FJD. Fundación Hispana de Osteoporosis y Metabolismo Mineral (FHOEMO). Madrid. España

**Dr. Adolfo Díez Pérez**

Universidad de Barcelona. Servicio de Medicina Interna. Instituto Municipal de Investigación Médica. (IMIM). Hospital del Mar. Barcelona. España

**Dr. Oswaldo Daniel Messina**

Facultad de Medicina. Universidad de Buenos Aires. Hospital Cosme Argerich. Buenos Aires. Argentina

**Dra. María Jesús Gómez de Tejada Romero**  
(*Editor Head*)

Universidad de Sevilla. Departamento de Medicina. Sevilla. España

**Dr. Manuel Sosa Henríquez**

(*Director*)  
Universidad de Las Palmas de Gran Canaria. Grupo de Investigación en Osteoporosis y Metabolismo Mineral. Hospital Universitario Insular. Servicio de Medicina Interna. Unidad Metabólica Ósea. Las Palmas de Gran Canaria. España

**Committee of experts**

Pilar Aguado Acín  
Javier Alegre López  
María José Américo García  
Abdón Arbelo Rodríguez  
Miguel Arias Paciencia  
Emilia Aznar Villacampa  
Chesús Beltrán Audera  
Pere Benito Ruiz  
Santiago Benito Urbina  
Miguel Bernard Pineda  
Pedro Betancor León  
Josep Blanch i Rubió  
José Antonio Blázquez Cabrera  
José Ramón Caeiro Rey  
Javier Calvo Catalá  
M<sup>a</sup> Jesús Cancelo Hidalgo  
Jorge Cannata Andía  
Antonio Cano Sánchez  
Cristina Carbonell Abella  
Jordi Carbonell Abelló  
Pedro Carpintero Benítez  
Enrique Casado Burgos  
Santos Castañeda Sanz  
Fidencio Cons Molina  
Sonia Dapia Robleda  
Bernardino Díaz López  
Casimira Domínguez Cabrera  
Anna Enjuanes Guardiola  
Pedro Esbrit Argüelles  
Fernando Escobar Jiménez  
José Filgueira Rubio  
Jordi Fiter Areste  
Juan José García Borrás  
Juan Alberto García Vadillo  
Eduardo Girona Quesada  
Carlos Gómez Alonso  
Milagros González Béjar  
Jesús González Macías  
Emilio González Reimers  
Jenaro Graña Gil  
Silvana di Gregorio  
Daniel Grinberg Vaisman  
Nuria Guañabens Gay  
Roberto Güerri Fernández  
Federico Hawkins Carranza  
Diego Hernández Hernández  
José Luis Hernández Hernández  
Gabriel Herrero-Beaumont Cuenca  
Esteban Jódar Gimeno

Fernando Lecanda Cordero  
Pau Lluch Mezquida  
José Andrés López-Herce Cid  
M<sup>a</sup> Luisa Mariñoso Barba  
Guillermo Martínez Díaz-Guerra  
María Elena Martínez Rodríguez  
Julio Medina Luezas  
Leonardo Mellivobsky Saldier  
Manuel Mesa Ramos  
Pedro Mezquita Raya  
Ana Monegal Brancos  
Josefa Montoya García  
María Jesús Moro Álvarez  
Manuel Muñoz Torres  
Laura Navarro Casado  
Manuel Naves García  
José Luis Neyro Bilbao  
Xavier Nogués i Solán  
Joan Miquel Nolla Solé  
José Antonio Olmos Martínez  
Norberto Ortego Centeno  
Santiago Palacios Gil-Antuñano  
Esteban Pérez Alonso  
Ramón Pérez Cano  
José Luis Pérez Castrillón  
Luis Pérez Edo  
Pilar Peris Bernal  
Concepción de la Piedra Gordo  
José Manuel Quesada Gómez  
Enrique Raya Álvarez  
Rebeca Reyes García  
José Antonio Riancho Moral  
Luis de Rio Barquero  
Luis Rodríguez Arboleya  
Minerva Rodríguez García  
Antonia Rodríguez Hernández  
Manuel Rodríguez Pérez  
Montaña Román García  
Inmaculada Ros Villamajó  
Rafael Sánchez Borrego  
Armando Torres Ramírez  
Antonio Torrijos Eslava  
Carmen Valdés y Llorca  
Carmen Valero Díaz de Lamadrid  
Ana Weruaga Rey  
Jaime Zubieta Tabernero  
**METHODOLOGY AND DESIGN OF DATA**  
Pedro Saavedra Santana  
José María Limiñana Cañal

**Volume 4 reviewers (2012)**

Bernardino Díaz López	José Antonio Blázquez Cabrera	M <sup>a</sup> Jesús Gómez de Tejada Romero
José Luis Hernández Hernández	José Antonio Riancho Moral	Xavier Nogués i Solán
Juan José García Borrás	José Luis Pérez Castrillón	Jenaro Graña Gil
Federico Hawkins Carranza	Ana Monegal Brancós	Pau Lluch Mezquida
Manuel Mesa Ramos	Manuel Naves Díaz	Carlos Gómez Alonso
Norberto Ortego Centeno	Daniel Grinberg Vaisman	Diego Hernández Hernández
Javier del Pino Montes	Ana Weruaga Rey	Silvana di Gregorio
Enrique Casado Burgos	Laura Navarro Casado	Minerva Rodríguez García
M <sup>a</sup> Luisa Mariñoso Barba	Jordi Carbonell Abelló	Rebeca Reyes García
Sonia Dapia Robleda	José Luis Neyro Bilbao	Esteban Pérez Alonso
Beatriz González López de Valcárcel	M <sup>a</sup> Jesús Cancelo Hidalgo	Ernesto Cannalis
Pedro Saavedra Santana	Guillermo Martínez-Díaz Guerra	Ramón Pérez Cano
Manuel Sosa Henríquez	Pilar Peris Bernal	Roberto Carlos Güerri Fernández
Mario Vicente Barrero	Manuel Sosa Henríquez	Gabriel Herrero-Beaumont Cuenca

*The Board of Directors and Management SEIOMM Magazine thanks you for your invaluable assistance.*

# Sclerostin and bone in diabetes mellitus type 2

**Jódar Gimeno E**

Jefe del Servicio de Endocrinología y Nutrición Clínica - Hospital Universitario Quirón - Madrid

Correspondence: Esteban Jódar Gimeno - Hospital Universitario Quirón - C/Diego de Velázquez, 1 - 28223 Pozuelo de Alarcón - Madrid (Spain)  
e-mail: ejodar.mad@quiron.es

**I**n the current number, García-Martín et al.<sup>1</sup> from the working group of Dr. Muñoz of Granada report that blood levels of sclerostin – the protein coded for by the gene SOST, which inhibits the osteoblast Wnt pathway - depend on the sex, the age and the renal function of patients with diabetes mellitus type 2 (DM2). They also demonstrate, contrary to expectations, a negative relationship with the markers for bone remodelling, and a positive relationship with bone mineral density (BMD). Finally, they show that blood levels of sclerostin are lower in patients with DM2 and osteoporosis irrespective of the presence or absence of fractures.

DM2 is a disease of high prevalence – up to 12-15% of the adult population in our country<sup>2</sup> - and with an enormous impact on morbi-mortality and quality of life. Its relationship with micro-vascular complications – retinopathy, nephropathy and diabetic neuropathy – and macro-vascular complications – coronary artery, peripheral arterial and cerebrovascular disease - is well known. Most recently, new complications have been recognised to be clearly related to diabetes, among which osteoporosis or diabetes-related metabolic bone disease is a notable example.

Metabolic bone disease in subjects with DM2 is characterised by the presence of an increased average bone mineral density (BMD) in spite of which the number of fractures – especially appendicular – is clearly higher than expected. Obviously, this situation has been interpreted as a change in bone quality, that is, in the characteristic materials and structures of the bone tissue, related more or less directly with the chronic hyperglycemia from which those with DM suffer<sup>3</sup>. Hence, the work of García-Martín et al.<sup>1</sup> may indicate that the increase in sclerostin in subjects with DM2 results in a reduction in remodelling which, although reducing bone loss and increasing BMD, results in bone which is less biomechanically effective. On the other hand, over the last decade

the skeleton has been shown to have new and unexpected functions in relation to the rest of the organism. We have assisted in this process in the discovery and characterisation of fibroblast growth factor 23 (FGF23), basically produced by the osteocytes, not only as a phosphaturic factor, but also a hormone originating in the bone-inhibiting calcitropic hormones – PTH and D-<sup>4</sup> hormone.

Among these new functions is emerging the role of bone tissue in the control of energy metabolism which happens through the secretion of osteocalcin (BGP), which we should also consider to be a hormone produced by osteoblasts, which regulates the secretion of insulin, sensitiveness to insulin and the use of energy. The signalling pathway for insulin in the osteoblasts (OB) drives glucose homeostasis in the body, the negative regulation of the carboxylation of BGP and its bioavailability, showing a typical negative hormonal feedback. The insulin signal in the OBs stimulates not only the acquisition of post-natal bone, but also bone resorption through the sympathetic system<sup>5,6</sup>. Also, leptin – an anorexigenous adipokine secreted following the acquisition of fatty acids by the adipocytes – which acts on the hypothalamus, also influences the carboxylation of BGP and, therefore, regulates bone and hydrocarbon metabolism<sup>7</sup>. The work collected in this number suggests a role of sclerostin in the appearance of bone disease in DM2. Other contributions from the same group have demonstrated the presence of higher concentrations of sclerostin in subjects with DM2 in comparison with controls which, in addition to being related to BMD and markers for bone remodelling, are correlated with the period of time over which the diabetes has developed and with glycaemic control (measured as HbA1c)<sup>8</sup>.

So, this research demonstrates that sclerostin is increased in subjects with DM2, correlated with the duration and control of the disease, which makes this molecule, at the very least, a potential mediator in the genesis of diabetes-related bone disease. Its exact role among other hormone

mediators released by the bone (which we should start calling osteokines, if not bone hormones) is yet to be elucidated and, what is even more attractive, could bring us close to discovering the nexus between metabolic bone disease and the high cardiovascular risk in DM2.

### Bibliography

1. García-Martín A, Reyes-García R, Rozas-Moreno P, Varsavsky M, Luque-Fernández I, Avilés-Pérez MD, et al. Variables que influyen en las concentraciones de esclerostina en los pacientes con diabetes mellitus tipo 2 y su asociación con el metabolismo óseo. *Rev Osteoporos Metab Miner* 2012 [Epub ahead of print].
2. Soriguer F, Goday A, Bosch-Comas A, Bordiú E, Calle-Pascual A, Carmena R, et al. Prevalence of diabetes mellitus and impaired glucose regulation in Spain: the Di@bet.es Study. *Diabetología* 2012;55:88-93.
3. Leslie WD, Rubin MR, Schwartz AV, Kanis JA. Type 2 diabetes and bone. *J Bone Miner Res* 2012;27:2231-7.
4. Bergwitz C, Jüppner H. Regulation of phosphate homeostasis by PTH, vitamin D, and FGF23. *Annu Rev Med* 2010;61:91-104.
5. Clemens TL, Karsenty G. The osteoblast: an insulin target cell controlling glucose homeostasis. *J Bone Miner Res* 2011;26:677-80.
6. Schwetz V, Pieber T, Obermayer-Pietsch B. The endocrine role of the skeleton: background and clinical evidence. *Eur J Endocrinol* 2012;166:959-67.
7. Confavreux CB. Bone: from a reservoir of minerals to a regulator of energy metabolism. *Kidney Int* 2011;121(Suppl.):S14-9.
8. García-Martín A, Rozas-Moreno P, Reyes-García R, Morales-Santana S, García-Fontana B, García-Salcedo JA, et al. Circulating Levels of Sclerostin Are Increased in Patients with Type 2 Diabetes Mellitus *J Clin Endocrinol Metab* 2012;97:234-41.

García-Martín A<sup>1</sup>, Reyes-García R<sup>1</sup>, Rozas-Moreno P<sup>1,2</sup>, Varsavsky M<sup>3</sup>, Luque-Fernández I<sup>4</sup>, Avilés-Pérez MD<sup>1</sup>, Muñoz-Torres M<sup>1,5</sup>

1 Unidad de Metabolismo Óseo, Endocrinología y Nutrición - Hospital Universitario San Cecilio - Granada

2 Servicio de Endocrinología - Hospital General de Ciudad Real - Ciudad Real

3 Servicio de Endocrinología - Hospital San Pau i Santa Tecla - Tarragona

4 Servicio de Endocrinología y Nutrición - Hospital Virgen de la Salud - Toledo

5 Plataforma de Metabolismo Mineral y Óseo (RETICEF) - España

## Variables which influence concentrations of sclerostin in patients with diabetes mellitus type 2 and its association with bone metabolism

Correspondence: Antonia García-Martín - Servicio de Endocrinología y Nutrición - Hospital Universitario San Cecilio - Avda. Dr. Oloriz, 16 - 18012 Granada (Spain)  
e-mail: garciamartin\_t@hotmail.com

Date of receipt: 19/05/2012

Date of acceptance: 15/08/2012

SEIOMM work scholarship to attend the 34th Congress ASBMR (San Diego, California, 2011)

### Summary

**Background and objectives:** Diabetes mellitus type 2 (DM2) is associated with an increased risk of fractures whose underlying mechanisms are complex. The objective of this study was to analyse the variables which influence blood concentrations of sclerostin and the relationship with bone metabolism in a group of DM2 patients.

**Patients and methods:** A transversal study of 76 patients with DM2. Clinical data, basic biochemical parameters, calciotropic hormones, markers for bone remodelling, vertebral X-rays and bone mineral density (BMD) were gathered. Blood concentrations of sclerostin were determined using ELISA (Biomedica, Austria).

**Results:** The males had higher concentrations than the females ( $63.15 \pm 27.03$  vs  $43.14 \pm 17.08$  pmol/L,  $p < 0.001$ ). We found positive relationships between sclerostin and age in males with DM2 ( $r = 0.338$ ,  $p = 0.031$ ) and between sclerostin and creatinine in the whole sample (adjusted for age:  $r = 0.362$ ,  $p < 0.001$ ). Also, it had a negative relationship with bone alkaline phosphatase (BAP) ( $r = -0.259$ ,  $p = 0.029$ ), carboxy-terminal telopeptide of type 1 collagen (CTX) ( $r = -0.356$ ,  $p = 0.002$ ) and tartrate-resistant acid phosphatase 5 $\beta$  (TRAP $\beta$ ) ( $r = -0.289$ ,  $p = 0.013$ ). BMD in the lumbar spine, femoral neck and total hip were positively associated with sclerostin ( $r = 0.373$ ,  $r = 0.492$ ,  $r = 0.524$ ,  $p < 0.001$ ) adjusted for age. Blood levels of sclerostin were lower in patients with DM2 and osteoporosis than those who were non-osteoporotic ( $42.96 \pm 19.16$  vs  $56.95 \pm 25.98$  pmol/L,  $p = 0.041$ ).

**Conclusions:** Sex, age and renal function are determining factors of levels of sclerostin in the circulation of patients with DM2. There is a negative relationship with remodelling markers and a positive one with BMD. Blood levels of sclerostin are lower in patients with DM2 and osteoporosis.

**Key words:** sclerostin, diabetes mellitus type 2, bone metabolism.

**Abbreviations:** FN: femoral neck; LS: lumbar spine; TH: total hip; CTX: carboxy-terminal telopeptide of type 1 collagen; DXA: dual X-ray absorptiometry; BAP: bone alkaline phosphatase; GF: glomerular filtration; BBG: basal blood glucose; HbA1c: glycated haemoglobin; BMI: body mass index; PTH: parathormone; OC: osteocalcin; TRAP $\beta$ : tartrate-resistant acid phosphatase 5 $\beta$ ; 25(OH)D: 25-hydroxyvitamin D.

## Introduction

Osteoporosis and diabetes mellitus are two highly prevalent diseases which are associated with an increased risk of fragility fractures, and a substantial impact on the morbidity and mortality of the general population. While various observational studies have investigated the association between the two, the mechanism by which diabetes favours the appearance of fractures does not appear to have been established adequately. The discovery of the Wnt pathway, which stimulates the differentiation of osteoblast precursors, has meant a recent advance in the understanding of bone homeostasis<sup>1</sup>. Thus, the role of this signalling pathway and its antagonists may be crucial in the pathogeny of the alterations in bone quality seen in diabetes mellitus.

The data published from animal experiments centre on an analysis of gene expression and the concentration in the bone microenvironment of some of the proteins involved. In fact, a study in mice with diabetes mellitus type 1 (DM1) induced by streptozotocin showed suppression of the gene expression for sclerostin, an increase in osteocyte apoptosis and low concentrations of total and nuclear  $\beta$ -catenin<sup>2</sup>. On the other hand, Nuche-Berenguer et al. showed that the gene expression for Dkk1 and SOST in models of mice with DM2 were found to be suppressed, while in models of insulin-resistant mice there was evidence of gene overexpression of SOST associated with an increase in levels of mRNA for LRP5<sup>3</sup>.

Previously, we have reported that levels of sclerostin were found to be raised in patients with diabetes mellitus type 2 (DM2)<sup>4</sup>, coinciding with the findings of Nuti et al.<sup>5</sup>. The aim of our study was to analyse the variables which influence blood concentrations of sclerostin and the relationship with bone metabolism in a group of patients with DM2.

## Patients and methods

### *Study population*

Our study, of a transversal nature, included a group of patients with DM2 diagnosed according to the criteria of the American Diabetes Association<sup>6</sup>. They were recruited consecutively from January 2006 to December 2007 in the endocrinology and nutrition clinic of the University Hospital San Cecilio of Granada.

All the patients met the following inclusion criteria: Caucasian, mobile, aged between 35 and 65 years and with normal haemogram, creatinine, liver function, calcium and phosphorus values. The exclusion criteria were: chronic disease except DM2, conditions which affect bone metabolism (Paget's disease, rheumatoid arthritis, hyperparathyroidism, hypercortisolism, malignant tumours, transplant) and treatment with drugs which interfere in bone metabolism (calcium supplements, vitamin D preparations, selective estrogen receptor modulators, calcitonin, estrogen therapy, antiresorptives, thiazides, glucocorticoids or anticonvulsants).

The study was carried out with the approval of the ethics committee of the hospital and adjusted according to the relevant directives for research in humans. All the patients signed their informed consent for their inclusion.

### *Analytical determinations*

Basal blood glucose (BBG), glycated haemoglobin (HbA1c), calcium, phosphorus and creatinine were measured using automated laboratory techniques. The glomerular filtrate rate (GF) was estimated using the Cockcroft-Gault equation. The blood levels of parathormone (PTH immunoassay, Roche Diagnostics SL, Bracelona, Spain) and 25-hydroxyvitamin D (25-OH-D, radioimmunoassay, DiaSorin, Stillwater, Minnesota, US).

The remodelled bone markers for formation collected were: osteocalcin (OC, radioimmunoassay, DiaSorin, Minnesota, US) and bone alkaline phosphatase (BAP) (BAP, ELISA, Tandem-R Ostase TM, Hybritech Europe, Liege, Belgium). The markers for resorption were: tartrate-resistant acid phosphatase 5 $\beta$  (TRAP $\beta$ , colourimetry, Hitachi 704 Boehringer Mannheim GmbH) and carboxy-terminal telopeptide of type 1 collagen (CTX, enzymatic immunoassay, analyser Elecsys Crosslaps, Roche Diagnostics SL, Barcelona, Spain).

Blood levels of sclerostin were measured using ELISA (Biomedica, Austria). In our laboratory, two samples with a known concentration were tested 6 times to calculate the intratrial variability which was 4% and two samples of known concentration were tested to calculate the intertrial variability which was 3%. The measurement of sclerostin was expressed in picomoles per litre (pmol/L) and the minimum detection level was <10 pmol/L.

### *Bone mineral density and vertebral X-ray study*

The bone mineral density (BMD) of the lumbar spine (LS) L2-L4, femoral neck (FN) and total hip (TH) were determined in all patients using dual X-ray absorptiometry (DXA) using the Hologic® QDR-4500 densitometer (Whatman, MA; coefficient of variation <1%). All the measurement were made by the same operator. We used the criteria of the World Health Organisation (WHO) for the diagnosis of osteoporosis<sup>7</sup>. Simple X-rays (XR) were also carried out of the dorsal and lumbar spine for the analysis of morphometric vertebral fractures and were interpreted in accordance with the algorithm developed by Genant et al.<sup>8</sup>.

### *Statistical analysis*

The statistical analysis of the data was carried out using the SPSS programme (version 15.0, Chicago, US). For continuous variables, the Kolmogorov-Smirnoff test was used to evaluate if they would follow a normal distribution. Measures of central tendency (mean) and dispersion (standard deviation, range) for continuous variables, and distribution of absolute and relative frequencies for categorical variables, were used. The differences for the variables of interest between com-

Table 1. Characteristics of the study sample

	n=76	Men n=41	Women n=35
Age (years)	57.9±6.5	57.4±6.8	58.6±6.1
BMI (kg/m <sup>2</sup> )	31.3±5.7	29.8±4.4	33±6.6
Duration diabetes (years)	13.4±7.5	13.2±6.7	13.6±8.5
Serum parameters:			
- BBG (mg/dL)	174.8±62.9	177±65.3	172.3±60.9
- HbA1c (%)	8±1.9	8.1±2	7.9±1.8
- Creatinine (mg/dL)	0.9±0.2	0.8±0.3	1±0.1
- GFO (ml/min/1.73 m <sup>2</sup> )	93.4±26.9	95.8±29.5	92.3±24.3
- Calcium (mg/dL)	9.6±0.5	9.6±0.5	9.4±0.5
- Phosphorus (mg/dL)	3.7±0.6	3.6±0.6	3.8±0.4
- PTH (pg/mL)	38.7±18.4	33.5±15.2	43.8±20
- 25(OH)D (ng/mL)	17.6±11.2	17.6±10.1	18.1±12.5
- OC (ng/mL)	1.45±1.27	1.35±1.19	1.62±1.33
- BAP (µg/L)	14.8±6.5	13.4±4.2	16.6±8.3
- CTX (ng/mL)	0.212±0.13	0.163±0.082	0.264±0.14
- TRAP $\beta$ (UI/L)	1.38±1	1.26±0.96	1.56±1.02
- Sclerostin (pmol/L)	53.93±24.95	63.15±27.03	43.14±17.08
Parameters DXA:			
- BMD CL (g/cm <sup>2</sup> )	0.949±0.142	0.963±0.131	0.932±0.153
- BMD CF (g/cm <sup>2</sup> )	0.818±0.13	0.861±0.131	0.766±0.109
- BMD CT (g/cm <sup>2</sup> )	0.905±0.142	0.942±0.145	0.859±0.127
- T-score CL	-1.3±1.3	-1.375±1.218	-1.317±1.452
- T-score CF	-0.59±1	-0.461±1.052	-0.758±0.981
- T-score CT	-0.61±1	-0.568±1	-0.661±1.03
Osteoporosis (%)	19.7	9.2	10.5
Vertebral fractures (%)	26.3	18.4	7.9

BMI: body mass index; BBG: baseline blood glycemia; HbA1c: glycated haemoglobin; GFO: glomerular filtration index; PTH: parathormone; 25(OH)D: 25-hydroxyvitamin D; OC: osteocalcin; BAP: bone alkaline phosphatase; CTX: carboxy-terminal telopeptide of type 1 collagen; TRAP $\beta$ : tartrate-resistant acid phosphatase 5 $\beta$ ; BMD: bone mineral density; LS: lumbar spine; FN: femoral neck; TH: total hip.

parison groups were carried out using Student's t-test for two independent samples and the Mann-Whitney U-test in the case of continuous variables. For categorical variables Pearson's chi squared test and Fisher's exact test were used. The relationship between the quantitative variables was analysed using Pearson's or Spearman's bivariate correlation test. To control the effect of one or more variables on the Pearson correlation coefficient the partial correlation test was used. All the statistical

tests were carried out as two-tailed. A value of  $p < 0.05$  was considered to be statistically significant.

## Results

Table 1 shows the clinical, biochemical and densitometric characteristics of the whole sample, and according to sex. The diabetic women had a body mass index ( $p=0.016$ ), blood levels of PTH ( $p=0.01$ ) and CTX ( $p<0.001$ ) greater than the men,

Figure 1. Blood levels of sclerostin as a function of sex

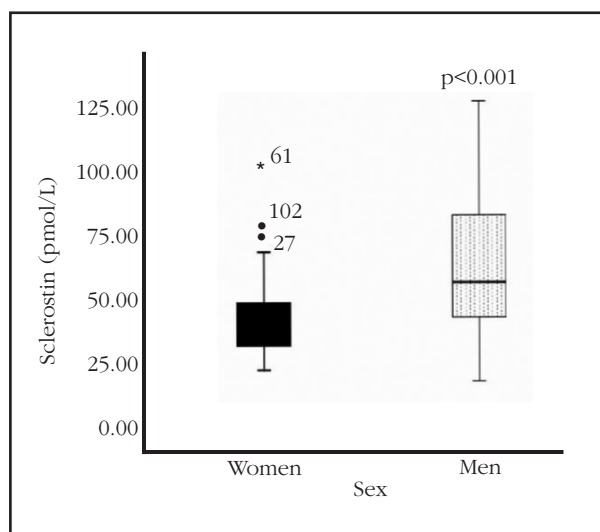
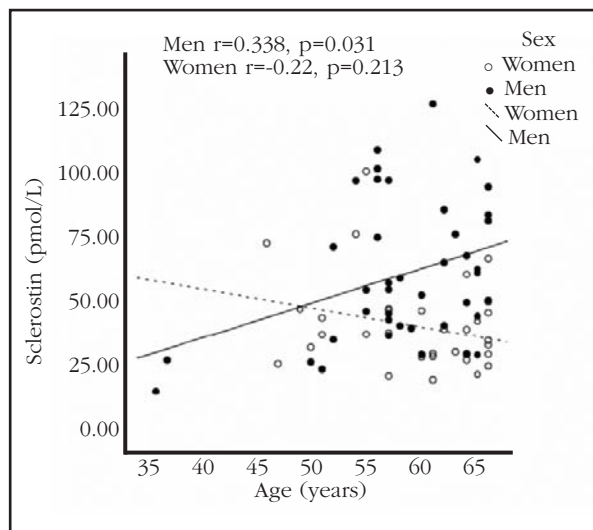


Figure 2. Correlation between sclerostin and age



while the men had a higher BMD in the femoral neck ( $p=0.002$ ) and in the total hip ( $p=0.015$ ) compared with the women. There were no differences in the rest of the variables.

The men had higher concentrations of sclerostin than the women ( $63.15 \pm 27.03$  as opposed to  $43.14 \pm 17.08$  pmol/L,  $p < 0.001$ ) (Table 1 and Figure 1). In the males, the levels of sclerostin were positively correlated with age ( $r=0.333$ ,  $p=0.031$ ), but this relationship did not hold for women ( $r=0.223$ ,  $p=0.213$ ) (Figure 2).

In the total sample blood levels of sclerostin showed a positive correlation with values of creatinine in the blood ( $r=0.37$ ,  $p < 0.001$ ) and negative, although not statistically significantly, with glomerular filtrate ( $r=-0.184$ ,  $p > 0.05$ ). After adjusting for age this relationship remained significant for blood levels of creatinine ( $r=0.361$ ,  $p=0.001$ ).

The levels of sclerostin were negatively correlated with the marker for bone formation BAP ( $r=-0.277$ ,  $p=0.021$ ) and with the markers for bone resorption CTX ( $r=-0.363$ ,  $p=0.002$ ) and TRAP $\beta$  ( $r=-0.276$ ,  $p=0.02$ ). There was no relationship with the marker for formation OC (Figure 3).

BMD and T-score in the lumbar spine, femoral neck and total hip were positively related with levels of sclerostin after adjusting for age (Table 2).

In patients with osteoporosis the levels of sclerostin were significantly lower than the non-osteoporotic patients ( $44.03 \pm 19.41$  pmol/L as opposed to  $56.95 \pm 25.98$  pmol/L,  $p=0.048$ ) (Figure 4). However there was no relationship with morphometric fractures ( $54.03 \pm 26.55$  as opposed to  $53.72 \pm 23.27$  pmol/L,  $p > 0.05$ ).

## Discussion

The levels of sclerostin were found to be increased in males. These results coincide with those described in a broad populational cohort study of 362 women and 318 men in which the women,

whether they were pre- or postmenopausal, had lower levels of sclerostin than the men<sup>9</sup>. The authors postulate that the larger size of the skeleton, around 21% greater in males, may explain the gender differences in blood concentrations of sclerostin. On the other hand, Mödder et al. maintain that the estrogens influence and regulate the synthesis of sclerostin, basing the differences observed on the levels of sclerostin among pre- and postmenopausal women, these being lower in the former, and on an earlier study in which treatment with estrogens in postmenopausal women reduced levels of sclerostin by 27%<sup>10</sup>. Molecular studies support the estrogenic role in the regulation of bone mass through the Wnt pathway by means of the  $\alpha$  estrogen receptor which is involved in the transport to the nucleus of  $\beta$ -catenin in response to the mechanical tension of the osteocyte<sup>11</sup>.

We observed an increase in blood levels of sclerostin with age in males. The influence of age on levels of sclerostin is being studied in depth. It is known that the expression of the Wnt pathway proteins by the osteoblast are regulated individually by age<sup>12</sup>, and a number of clinical studies have confirmed this relationship in both men and women<sup>9,13</sup>. Hence, a population study carried out in 1,235 premenopausal, and 568 postmenopausal women in an age range from 20 to 79 years, analysed the changes in blood concentrations of sclerostin with age. One of the conclusions was that between 35 and 45 years of age the levels of sclerostin remained stable, and from 45 years of age they increased progressively<sup>14</sup>. Some authors postulate that the production of sclerostin in each osteocyte increases with age, while not excluding the possibility that their clearance is reduced.

Although the way sclerostin is eliminated is not known, the most probable option, given the size and weight of this protein, is that it is eliminated in the kidney. In our study the levels of sclerostin

were positively related with blood concentrations of creatinine and negatively with glomerular filtrate. These results coincide with earlier works which show that levels of sclerostin increase with a deterioration of renal function, above all in chronic renal insufficiency grade 3 or higher, and with no relationship to hepatic function<sup>15</sup>. Similarly, in patients with chronic renal disease in haemodialysis levels of sclerostin are higher than those of controls<sup>16</sup>.

In theory, raised concentrations of sclerostin ought to be associated with a decrease in markers for bone formation. However, we found that levels of sclerostin in patients with diabetes were negatively related with both markers for formation (BAP) and resorption (CTX and TRAP). Similarly, in women over the age of 60 years levels of sclerostin were negatively associated with blood levels of BAP and amino-terminal propeptide of type 1 collagen (P1NP), as well as CTX<sup>9</sup>. In patients immobilised after a stroke blood sclerostin was negatively correlated with BAP and positively with CTX<sup>17</sup>. On the other hand, other studies found no relationship between sclerostin and markers for bone remodelling<sup>13,16,18,19</sup>. Therefore, we consider that the data regarding sclerostin and markers for bone remodelling are contradictory and do not allow definitive conclusions to be drawn.

Bone mass, expressed as BMD, T-score and Z-score, are positively related with levels of sclerostin, both in the group with DM2 as well as in the control group in our study. Similarly, BMD was the main predictive variable for blood concentration of sclerostin. These findings differ from those observed in patients with sclerosteosis or Van Buchem's disease<sup>20,21</sup> and in Knockout mice models for sclerostin or with overexpression of sclerostin<sup>22,23</sup>. Given that the physiological role of sclerostin is the inhibition of osteoblast proliferation and activity, what would be expected would be a negative relationship with bone mass. However, our results coincide with some other works in which this aspect is examined. Thus, in patients with renal insufficiency in haemodialysis levels of sclerostin were positively correlated both with BMD in the femoral neck, lumbar spine and radius, as well as with trabecular density and the number of trabeculae in the radius and tibia measured using high resolution peripheral computerised tomography (CT)<sup>16</sup>. In addition, the BMD and BMC (bone mineral content) in the lumbar spine and hip were positively related with the concentration of sclerostin in healthy subjects after adjusting for age, sex and renal function<sup>13</sup>. In the cohort of Mödder et al. a positive association was also found between total BMC and levels of sclerostin, but only significant from 40 years of age, and greater from 60 years of age<sup>9</sup>. Also, the levels of sclerostin were related positively with BMD in the distal femur and proximal tibia in patients with chronic medullar lesion<sup>24</sup>.

In agreement with earlier findings, levels of sclerostin were lower in patients with diabetes and

Figure 3. Correlation between sclerostin and markers for bone remodelling

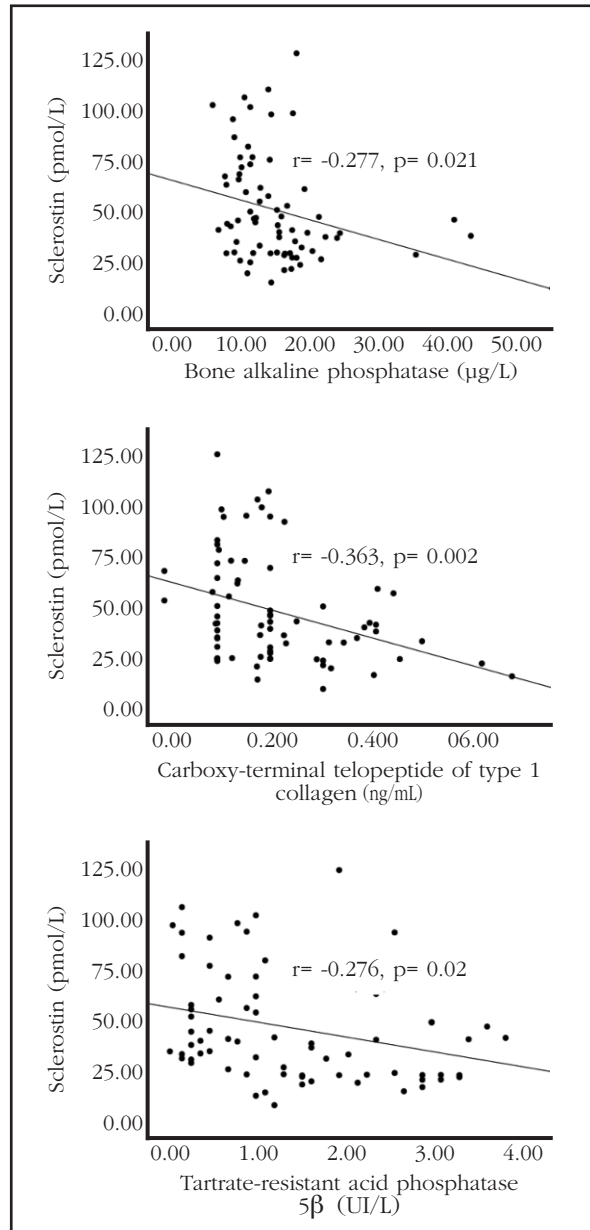


Figure 4. Blood levels of sclerostin as a function of diagnosis of osteoporosis

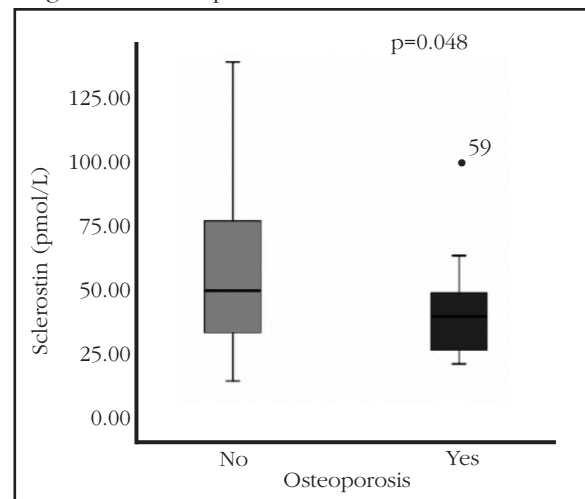


Table 2. Correlation between sclerostin, BMD, T-score and Z-score without adjustment and adjusted for age

	Simple	Adjusted for age
BMD CL (g/cm <sup>2</sup> )	r=0.337**	r=0.373**
T-score CL	r=0.285*	r=0.313*
Z-score CL	r=0.199	r=0.192
BMD CF (g/cm <sup>2</sup> )	r=0.487**	r=0.492**
T-score CF	r=0.405**	r=0.408**
Z-score CF	r=0.396**	r=0.391**
BMD CT (g/cm <sup>2</sup> )	r=0.505**	r=0.524**
T-score CT	r=0.406**	r=0.427**
Z-score CT	r=0.328**	r=0.323**

BMD: bone mineral density; LS: lumbar spine; FN: femoral neck; TH: total hip.

\* p<0.05

\*\* p<0.01

densitometric osteoporosis compared with those patients with diabetes but without densitometric osteoporosis. A similar relationship has been described between osteoporosis and sclerostin in women with postmenopausal osteoporosis to that which we found in patients with DM2<sup>19</sup>.

Various hypotheses have been suggested to explain the positive relationship between blood sclerostin and bone mass. The main one is that there are changes in the production of sclerostin by the osteocytes in relation to aging, with a higher production by each individual osteocyte<sup>9</sup>. On the other hand, the increase in the levels of sclerostin means a decrease in bone formation on the basis of its physiological functions, and therefore, allows there to be a drop in bone turnover. A lower bone turnover would mean slowed bone loss and higher bone mass<sup>16</sup>.

In summary, sex, age and renal function are determining factors in blood levels of sclerostin in patients with DM2. Similarly, we found a negative relationship with markers for bone remodelling and a positive relationship with BMD. Finally, blood levels of sclerostin are lower in patients with DM2 and osteoporosis, with no relationship to the presence of fractures.

**Conflict of interest:** There are no conflicts of interest on the part of the authors.

### Bibliography

- Baron R, Rawadi G. Wnt Signaling and the regulation of bone mass. *Curr Osteoporos Rep* 2007;5:73-80.
- Portal-Núñez S, Lozano D, de Castro LF, de Cortázar AR, Nogués X, Esbrit P. Alterations of the Wnt/beta-catenin pathway and its target genes for the N- and C-terminal domains of parathyroid hormone-related protein in bone from diabetic mice. *FEBS Lett* 2010;584:3095-100.
- Nuche-Berenguer B, Moreno P, Portal-Núñez S, Dapía S, Esbrit P, Villanueva-Peñacarrillo ML. Exendin-4 exerts osteogenic actions in insulin-resistant and type 2 diabetic states. *Regul Pept* 2010;159:61-6.
- García-Martín A, Rozas-Moreno P, Reyes-García R, Morales-Santana S, García-Fontana B, García-Salcedo JA, et al. Circulating levels of sclerostin are increased in patients with type 2 diabetes mellitus. *J Clin Endocrinol Metab* 2012;97:234-41.
- Nuti R, Valenti R, Merlotti D, Ceccarelli E, Ruvio M, Pietrini MG, et al. Circulating sclerostin levels and bone turnover in type 1 and type 2 diabetes. *J Clin Endocrinol Metab* 2012;97:1737-44.
- American Diabetes Association. Diagnosis and classification of Diabetes Mellitus. *Diabetes Care* 2005;28:S37-S42.
- Kanis JA, Melton LJ 3rd, Christiansen C, Johnston CC, Khaltsev N. The diagnosis of osteoporosis. *J Bone Miner Res* 1994;9:1137-41.
- Genant HK, Wu CY, van Kuijk C, Newitt MC. Vertebral fracture assessment using a semi-quantitative technique. *J Bone Miner Res* 1993;8:1137-48.
- Mödder UI, Hoey KA, Amin S, McCready LK, Achenbach SJ, Riggs BL, et al. Relation of age, gender, and bone mass to circulating sclerostin levels in women and men. *J Bone Miner Res* 2011;26:373-9.
- Mödder UI, Clowes JA, Hoey K, Peterson JM, McCready L, Oursler MJ, et al. Regulation of circulating sclerostin levels by sex steroids in women and in men. *J Bone Miner Res* 2011;26:27-34.
- Zaman G, Jessop HL, Muzylak M, De Souza RL, Pitsillides AA, Price JS, et al. Osteocytes use estrogen receptor alpha to respond to strain but their ERalpha content is regulated by estrogen. *J Bone Miner Res* 2006;21:1297-1306.
- Rauner M, Sipos W, Pietschmann P. Age-dependent Wnt gene expression in bone and during the course of osteoblast differentiation. *Age (Dordr)* 2008;30:273-82.
- Amrein K, Amrein S, Drexler C, Dimai HP, Dognig H, Pfeifer K, et al. Sclerostin and its association with physical activity, age, gender, body composition, and bone mineral content in healthy adults. *J Clin Endocrinol Metab* 2012;97:148-54.
- Ardawi MS, Al-Kadi HA, Rouzi AA, Qari MH. Determinants of serum sclerostin in healthy pre- and postmenopausal women. *J Bone Miner Res* 2011;26:2812-22.
- Kim SH, Lim HJ, Yoon SY, Lee SC, Lim SK, Rhee Y. Decreased renal function but not liver function overpowers the circulating sclerostin level. *American Society Bone Mineral*

- Research, 2011 Annual Meeting, SU0406.
16. Cejka D, Jäger-Lansky A, Kieweg H, Weber M, Bieglmayer C, Haider DG, et al. Sclerostin serum levels correlate positively with bone mineral density and microarchitecture in haemodialysis patients. *Nephrol Dial Transplant* 2012;27:226-30.
  17. Gaudio A, Pennisi P, Bratengeier C, Torrisi V, Lindner B, Mangiafico RA, et al. Increased sclerostin serum levels associated with bone formation and resorption markers in patients with immobilization-induced bone loss. *J Clin Endocrinol Metab* 2010;95:2248-53.
  18. Mirza FS, Padhi ID, Raisz LG, Lorenzo JA. Serum sclerostin levels negatively correlate with parathyroid hormone levels and free estrogen index in postmenopausal women. *J Clin Endocrinol Metab* 2010;95:1991-7.
  19. Polyzos SA, Anastasilakis AD, Bratengeier C, Woloszczuk W, Papatheodorou A, Terpos E. Serum sclerostin levels positively correlate with lumbar spinal bone mineral density in postmenopausal women-the six-month effect of risedronate and teriparatide. *Osteoporos Int* 2012;23:1171-6.
  20. Hamersma H, Gardner J, Beighton P. The natural history of sclerosteosis. *Clin Genet* 2003;63:192-7.
  21. Staehling-Hampton K, Proll S, Paeper BW, Zhao L, Charmley P, Brown A, et al. A 52-kb deletion in the SOST-MEOX1 intergenic region on 17q12-q21 is associated with van Buchem disease in the Dutch population. *Am J Med Genet* 2002;110:144-52.
  22. Li X, Ominsky MS, Niu QT, Sun N, Daugherty B, D'Agostin D, et al. Targeted deletion of the sclerostin gene in mice results in increased bone formation and bone strength. *J Bone Miner Res* 2008;23:860-9.
  23. Winkler DG, Sutherland MK, Geoghegan JC, Yu C, Hayes T, Skonier JE, et al. Osteocyte control of bone formation via sclerostin, a novel BMP antagonist. *EMBO J* 2003;22:6267-76.
  24. Morse LR, Sudhakar S, Danilack V, Tun C, Lazzari A, Gagnon DR, et al. Association between sclerostin and bone density in chronic SCI. *J Bone Miner Res* 2012;27:352-9.

Lozano D<sup>1</sup>, Trejo CG<sup>2</sup>, Manzano M<sup>3</sup>, Doadrio JC<sup>3</sup>, Salinas AJ<sup>3</sup>, Dapía S<sup>4</sup>, Caeiro Rey JR<sup>5</sup>, Gómez-Barrena E<sup>6</sup>, Vallet-Regí M<sup>3</sup>, García-Honduvilla N<sup>2</sup>, Buján J<sup>2</sup>, Esbrit P<sup>1</sup>

1 Laboratorio de Metabolismo Mineral y Óseo - Instituto de Investigación Sanitaria-Fundación Jiménez Díaz - Madrid

2 Departamento de Especialidades Médicas - Facultad de Medicina - Universidad de Alcalá - Alcalá de Henares - Madrid

3 Departamento de Química Inorgánica y Bioinorgánica - Facultad de Farmacia - Universidad Complutense - Madrid

4 Trabeculae S.L. - Orense

5 Complejo Hospitalario Universitario de Santiago de Compostela (CHUS) - Reticef - Santiago de Compostela

6 Departamento de Traumatología - Instituto de Investigación Sanitaria-Fundación Jiménez Díaz - Madrid

## Osteogenic effects of PTHrP (107-111) loaded in bioceramics in a model of bone regeneration after a cavitory defect in the femur of a rabbit

Correspondence: Daniel Lozano - Laboratorio de Metabolismo Mineral y Óseo - Instituto de Investigación Sanitaria-Fundación Jiménez Díaz - Avda. Reyes Católicos, 2 - 28040 Madrid (Spain)  
e-mail: dlozano@fjd.es

Date of receipt: 04/04/2012

Date of acceptance: 19/06/2012

*Working SEIOMM scholarship to attend the Congress of the ASBMR (Denver, 2009)*

### Summary

**Introducción:** Parathyroid hormone-related protein (PTHrP), which is abundant in bone tissue, is an important modulator of bone formation. It has been shown that PTHrP (107-111), called osteostatin, loaded into mesoporous ceramic material SBA-15 exerts osteogenic action *in vitro*.

**Objective:** To confirm if this material and a functionalised version of the same material (C8-SBA-15) promote bone regeneration in a model of a cavitory defect in a rabbit femur.

**Materials and methods:** Histological, immunohistochemical and computerised microtomography ( $\mu$ CT) studies were carried out in order to achieve the aims of the study.

**Results:** After the implantation of the biomaterials no significant levels of inflammation or bone resorption were observed (at 4 and 8 weeks). At 8 weeks the bioceramics not loaded with osteostatin were found to be separated from the bone medulla by a fibrous capsule which diminished significantly in the presence of the peptide. An increase was observed (using  $\mu$ CT) in bone neo-formation at different distances from the biomaterials, principally in those loaded with the osteostatin. These results were also confirmed by immunohistochemistry of osteoblast markers.

**Conclusion:** Our results suggest that the use of these osteostatin-loaded bioceramics are a good strategy for accelerating bone regeneration.

**Key words:** PTHrP, osteostatin, bioceramics, bone regeneration, cavitory defect.

## Introduction

The protein related to parathormone (PTHrP) was initially identified in tumorous hypercalcemia of humeral origin<sup>1</sup>. Currently, it is known that PTHrP and the type 1 receptor common to PTH/PTHrP (PTHR1) is expressed in a wide variety of tissues, malignant and non-malignant, in which PTHrP exerts auto/paracrine and intracrine effects<sup>2</sup>. Although the fragment 1-36 of PTHrP, which has a structural homology with PTH, exerts anabolic actions on bone, stimulating bone formation<sup>3-6</sup>, the possible mechanisms associated with this action are little understood. The C-terminal fragment of PTHrP is a powerful inhibitor of osteoclast activity<sup>7-10</sup>. In fact, the pentapeptide 107-111 of this protein (called osteostatin) has a powerful antiresorptive activity *in vitro* and *in vivo*<sup>11</sup>. Various *in vitro* studies have shown that osteostatin increases the differentiation of osteoblast cells in mice and in humans<sup>12-15</sup>, although its receptor in bone cells is not known<sup>9,16</sup>. A study made by our laboratory has shown that the native fragment of PTHrP which contains the sequence 107-139 rapidly transactivates the receptor 2 for the vascular endothelial growth factor (VEGF) in osteoblast cells<sup>17</sup>. On the other hand, it has been shown that the daily administration of this fragment of PTHrP over a period of two weeks in ovariectomised mice protects against bone loss observed in their large bones, with positive effects in cortical and trabecular bone<sup>3</sup>. Recently, our group has also shown that PTHrP (107-139) reverses osteopenia and increases the regeneration of bone in mice treated with 3-methylprednisolone or those which are diabetic<sup>18,19</sup>.

An understanding the regeneration mechanisms is fundamental to understanding the behaviour of bone tissue after the implant of a prosthesis or during the recuperation from a fracture. It is known that the process of bone repair in adults reproduces the normal development of the skeleton during embryogenesis<sup>20</sup>. Bone formation in the foetus starts with the condensation of mesenchymal cells followed by their differentiation to chondrocytes (endochondral ossification) or directly to osteoblasts (intramembranous bone formation). In the majority of fractures, the formation of the callus involves a combination of both types of ossification. Although the signalling pathways or the cellular interactions involved in the repair of bone are not completely known, there are different strategies to improve this process<sup>20</sup>. One of these involves the systemic or local application of osteogenic factors which increase the formation of fresh bone. It has been shown that daily injections of PTH improve the repair of bone in fracture in normal or ovariectomised rats<sup>21,22</sup>. In addition, the systemic administration of an analogue to PTHrP (1-34) counteracts the deleterious effects in a defect in the ulna of rabbits treated with prednisolone<sup>23</sup>. A more direct approach to increase bone repair would consist of a local release of osteogenic factors with biomaterials in the affected zone.

Biomaterials may be defined as "implantable materials which develop their function in contact

with living tissues"<sup>24</sup>. Recently, bioactive mesoporous ceramics have been designed which allow the adsorption and release of different molecules, with good prospects for clinical application<sup>25</sup>. The SBA (Santa Barbara Amorphous)-15 has a hexagonal structure of porous cylinders with a diameter of 5-10 nm. An advantage of this type of ceramic is its great porous volume and its concentration of SiOH groups<sup>26-28</sup>. In addition, this material has a series of interconnected micropores which promote greater ionic diffusion triggering a stronger bioactive response. In fact, the capture and release of L-tryptophan loaded into the SBA-15 material, and in a functionalised version (C8-SBA-15), has been studied<sup>29</sup>. The hydrophobic surface of the C8-SBA-15 material is capable of interacting with the indole ring of the tryptophan of different peptides and leaving smaller available space, occupied by alkyl chains. Our group has characterised the capture/release of osteocalcin loaded into these materials, demonstrating that the peptide confers on them osteogenic activity in osteoblasts in mice<sup>14</sup>.

The aim of the current study was to evaluate the capacity of the ceramic material SBO-15, functionalised or not with C8 groups (C8-SBA-15), loaded with PTHrP (107-111), to induce osteogenesis in a model of a cavity defect in a rabbit femur.

## Materials and methods

### *Preparation of the materials*

The mesoporous material SBA-15 was synthesised using a method based on the use of a surfactant, as a directing agent for the structure, and tetraethyl orthosilicate (Sigma-Aldrich, St Louis, MO) as the source of the silica<sup>35</sup>. This structure was confirmed by X-ray diffraction (XRD) and N<sub>2</sub> adsorption analysis. The functionalisation of the silica was achieved using the post-synthetic method or anchorage grafting of an alkoxy silane, N-octyltriethoxysilane (C8, Sigma-Aldrich), as described<sup>30</sup>. This was confirmed using Fourier transform infrared electroscopy for elementary analysis. The resulting functionalised material contains 11% by weight (0.97 mmol/g) of organic fractions, which allows the calculation of the degree of functionalisation.

For the experiments both types of SBA-15 material were formed into 50 mg discs (6 x 2 mm) by uniaxial (1MPa) and isostatic (1MPa) pressure. The materials were exposed to ultraviolet radiation in a cell culture chamber (FLV120, Technology for Diagnosis and Research, Madrid), overnight for their sterilisation. The bond between the PTHrP (107-139) (Bacjchem, Bubendorf, Switzerland) and the material was made by immersion in a peptide solution (100nM) in 1 ml of saline phosphate buffer (SPB), pH 7.4 at 4° C with agitation for 24 hours<sup>31,32</sup>.

### *Production of the rabbit cavity defect*

White male New Zealand rabbits were used (Granja San Bernardo, Valencia, Spain) aged 24-30 weeks [n=2 for computerised microtomography ( $\mu$ CT) and 5 for histological studies]. These animals were housed individually in cages in the animal facilities of the Jiménez Díaz Foundation over

a period of two weeks. The animals had free access to water and a standard diet (Panlab, Reus, Spain) in a room kept at an ambient temperature with cycles of 12 hours of light and 12 hours of darkness. All the studies were carried out with the approval of the animal research committee of the Jiménez Díaz Foundation. The pain and suffering was minimised in accord with European rules.

The surgical intervention was carried out under general anaesthetic. The rabbit bone was shaved in both knees with a medium velocity drill (5 mm in diameter and 4-5 mm in depth) to create lateral and medial cavity defects<sup>33</sup>. Following this, the trial materials were implanted and the wounds sutured. The right lateral defect received the SBA-15 material without the peptide, and the right medial defect, the SBA-15 loaded with PTHrP (107-111). The left lateral femoral defect received the SBA-15 material functionalised with C8, while the biomaterial C8-SBA-15 loaded with PTHrP (107-111) was implanted in the left medial femoral defect. The animals were sacrificed at 4 and 8 weeks after these interventions. The femurs were distributed for histological and immunohistochemical tests and  $\mu$ CT analysis.

#### *Histology*

The rabbit femurs were fixed in p-formaldehyde at 4% in SPB at 4° C. The samples were decalcified (24 h) in Osteosoft (48/72 h) (Merk, Whitehouse Station, N.J.), dehydrated and embedded in paraffin. The histological analyses were carried out in sections of 8  $\mu$ m on a sagittal plane, deposited on preprepared slides with L-Lysine (Polylysine, Thermo, Watham, MA), and then stained with haematoxylin/eosin. Before the staining the samples were kept at 60° C for 6-24 hours to fix the tissues to the slides. They were deparaffinised by incubating them sequentially in xylol, ethanol at 100%, and 70%, and distilled water. After staining the samples were dehydrated and mounted in DPX resin (a mixture of distyrene, plasticiser and xylol). Two histological sections from each rabbit were used from a total of 2-4 rabbits per experimental group. All the evaluations of the samples were analysed by 3 independent observers.

#### *Immunohistochemistry*

The histological slices obtained from the bone samples were deparaffinised and rehydrated. Blocking and permeabilisation in bovine blood albumen at 4% (in SPB with 0.1% of Triton X-100) was carried out for 30 minutes at room temperature. Antibodies were used against osteocalcin (OC) (Santa Cruz Biotechnology, Santa Cruz, CA), VEGF (Abcam, Cambridge, MA) RAM11 (Dako) and TRAP (Santa Cruz Biotechnology), and a polyclonal antibody against sclerostin (R&D, Minneapolis, MN). The primary antibodies were incubated in a humidity chamber throughout the night at 4°C, except in the case of sclerostin which was incubated for two hours at room temperature (RT). In all the antibodies, except that for sclerostin, a secondary biotinylated antibody was used. It was incubated with alkaline extravidin-phosphatase com-

plex (dilution 1:200), for 60 minutes at RT and washed with 3 times with SPB for 5 minutes. In the case of sclerostin the secondary antibody was bonded with peroxidase, which was incubated for 1 hour at RT. Development was carried out by incubation with the chromogen substrate DAB for 10 minutes. A sample without primary antibody was always included as a negative control. The samples were contrasted with haematoxylin. The cells positive for the different antibodies were determined in 10 fields in the vicinity of the material. In the case of the osteocytes positive for sclerostin, these were quantified in 5 random fields in the cortical bone.

#### *Analysis of $\mu$ CT*

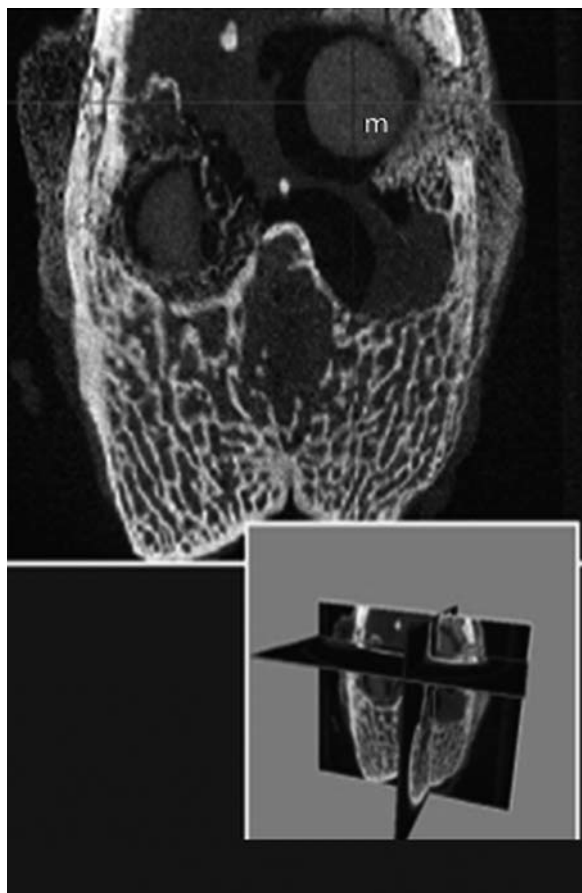
The samples of rabbit femur were cut with a hyperflexible disc of fine granulometry (15 $\mu$ m) and smooth abrasion connected to a surgical motor (KaVo, Dental GmbH, Biberach, Germany) at a velocity of 15,000 rpm. During the cutting process the sample was constantly irrigated with saline solution to prevent overheating and dehydration. The samples were scanned with a high resolution microtomography system (SkyScan 1172, Skyscan N.V., Aartselaar, Belgium), with an X-ray tube with a voltage of 100kV and a current of 100 $\mu$ A without filter. Once scanned, the images were generated using the DataViewer application (SkyScan), which were reconstructed according to the Feldkamp algorithm<sup>34</sup>. The angle of rotation of the scan was 360°. For the quantitative and qualitative analysis of bone growth around the implant the CTAn (SkyScan) application was used. From each sample a total of 70 images were analysed. The trabecular parameters were calculated in selected regions (Figure 1) between 0 and 5 pixels and 10 and 15 pixels, 1 pixel being the equivalent of 21.8  $\mu$ m. Using the CTVol application (SkyScan) three-dimensional models were created both of the biomaterial (which was considered to be a cylinder for better clarity of presentation) and the bone formed at different distances from the surface of the implant. The system of analysis provided the calculations of the following trabecular parameters:

- Percentage of bone volume (BV/TV): relates the volume of calcified bone tissue with respect to the total volume of the area analysed (%).
- Trabecular bone pattern factor (Tb,Pf): index of connectivity of trabecular bone. This is based on the principle that a greater trabecular concavity indicates greater connectivity, by increasing the probability of connection nodes between the trabeculae. Thus a lower Tb.Pf indicates a higher trabecular connectivity (mm<sup>-1</sup>).

#### *Statistical analysis*

The results are expressed as mean  $\pm$  standard error of the mean (SEM). The non-parametric comparison between two samples were carried out using the Mann Whitney test. Non-parametric ANOVA was used to compare various samples (Kruskal-Wallis) followed by a post-hoc test (Dunn). All values where  $p < 0.05$  were considered significant.

Figure 1. Computerised microtomography ( $\mu$ CT) image of rabbit distal femur with the biomaterial (m) incorporated



## Results

Histological techniques and  $\mu$ CT were used to confirm the response of the tissue to the biomaterial and the effect of the PTHrP (107-111) on the cavity defect in the rabbit femur, at 4 and 8 weeks.

From the histopathological analysis of the bone samples the following results were obtained:

### SBA-15

At 4 weeks from the implanting of the SBA-15 material, this was found to be intact, filling the cavity defect produced in the femur. The entry zone of the biomaterial was occupied by abundant dense connective tissue. Around the biomaterial was observed a large amount of osteoid (Figure 2A) in the cortical zones, and a fibrous capsule which isolated and enveloped the material, without apparently interfering with the medullar area. No inflammatory reaction was observed. At 8 weeks, the biomaterial in contact with the bone medulla did not have significant modifications, remaining isolated by the fibrous capsule. In addition, in the zone in contact with the cortical bone the formation of trabeculae was observed in the vicinity of the implant (Figure 4A).

### C8-SBA-15

In the animals implanted with this material a similar behaviour was observed to that described for the implant of non-functionalised SBA-15 after 4 weeks. However, the C8-SBA-15 was seen to be isolated by a fibrous capsule of greater thickness (Figure 2C). The bone repair seen at 8 weeks covered the whole cavity defect, with a well defined external fibrous capsule being observed surrounded by osteoid which occupied the entry space of the cavity of the biomaterial and newly-formed bone trabeculae surrounding the cortical face of the biomaterial (Figure 4C).

### SBA-15 + PTHrP (107-111)

At 4 weeks from the implant of the SBA-15 loaded with PTHrP (107-111) an intense scarring was observed which extended from the cavity to the entry of the biomaterial (now occupied by a thick layer of fibrous connective and articular cartilaginous tissue) with a great quantity of osteoid around it. The biomaterial in contact with the medullar area was seen to be surrounded by trabecular bone situated on the periphery of the osteoid surface (Figure 2B). On the other hand the osteoid described increased significantly around the cortical face of the biomaterial in the direction of the external surface at 8 weeks, while being, on the contrary, more limited towards the medullar zone where trabecular areas surrounding the implanted biomaterial were observed (Figure 4B).

### C8-SBA-15 + PTHrP (107-111)

The behaviour of the C8-SBA-15 loaded with PTHrP (107-111) was similar to that described in the last group, the fibrous capsule maintaining a greater thickness in comparison with the groups not functionalised with C8 (Figure 2D). At 8 weeks, during the process of repair, external connective hyperplasia, and hyperplasia of the hyaline cartilage, was observed, as well as bone hyperplasia which formed the tissue layer of the osteoid neoformations surrounding the implant. Most notable in this group was the internal reaction observed in the fibrous capsule, which appeared to be split, allowing the appearance of a space occupied by non-calcified osteoid which outlined the intact surface of the biomaterial (Figure 4D).

The observations carried out in the histological study at 4 and 8 weeks for each of the biomaterials were confirmed by  $\mu$ CT studies. In the representative images of each experimental group it is possible to see the bone formation again, with the presence of trabeculae, at different distances from the implanted material (Figures 3 and 5). The increase in bone formation observed in the images corresponding to the materials loaded with PTHrP (107-111) is evident from the increase in the BV/TV % and the reduction in Tb.Pf in the rabbit femur (Table 1).

The changes observed in the histology and the bone structure of the rabbit femur were correlated with a significant increase in staining of OC in the samples with materials loaded with PTHrP (107-

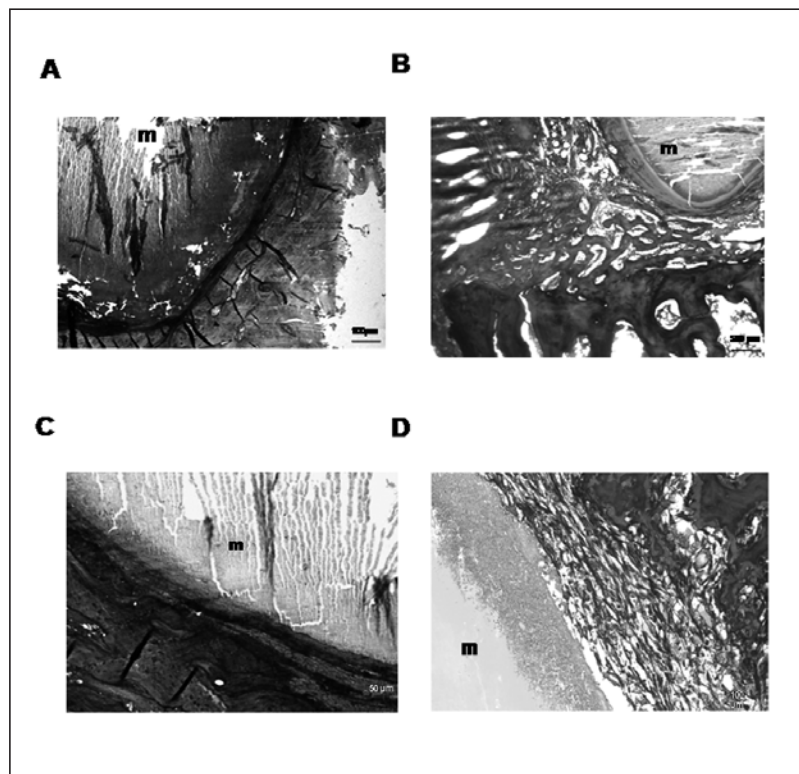
111) (Figure 6A). A significant increase was observed in the staining of femurs which contained the biomaterials loaded with PTHrP (107-111) in comparison with those which did not contain the peptide. It is especially worth noting that the presence of the peptide in the biomaterial C8-SBA-15 induced a greater effect in this marker than in the SBA-15 (Figure 6A). In none of the femurs studied was observed an increase in the inflammatory component in the presence of the different materials studied.

What is more, the presence of cells positive for the TRAP or RAM11 immunostain (Figures 6B and C) (macrophage marking) was very low in all the study groups (below 3%), and practically zero in the case of the materials with PTHrP (107-111). It was not possible to quantify the differences in positive immunostaining for VEGF (Figure 6D), since the marking was very faint for this marker in most of the study groups.

## Discussion

The results described above demonstrate the osteogenic capacity of osteostatin, loaded into ceramic materials SBA-15 and C8-SBA-15, in a bone regeneration model. These findings open new perspectives in the context of bone repair, since they suggest that local exposure to this pentapeptide in the bone environment would promote its regeneration. Recently, our group has demonstrated the capacity of the materials SBA-15 and C8-SBA-15 with PTHrP (107-111) to release the peptide into their environment, and it was observed that the former released approximately 4% more than the latter over time. This difference in release profile between the two materials is similar to that obtained with the same materials loaded with L-tryptophan, the C-terminal amino acid of PTHrP (107-111)<sup>29</sup>. It should be taken into account that the negative charges of SBA-15 at the physiological pH used in the process of capture of the peptide promote electrostatic interactions with the slightly positively charge of the amino groups in the PTHrP (107-111) at this pH. However, the hydrophobic surface of C8-SBA-15 is capable of interacting with the indole ring of the tryptophan in this peptide, although this functionalisation leaves a smaller available space (occupied by alkyl rings) for the adsorption of the peptide in the interior of the pores in comparison with SBA-15<sup>29</sup>. This may explain the fact that this material retains less PTHrP (107-111) than the C8-SBA-15.

Figure 2. Representative images of the Masson staining in rabbit femurs with implants of biomaterials SBA-15 (A) or C8-SBA-15 (C) loaded or not loaded (B and D respectively) with PTHrP (107-111) at 4 weeks after the cavity defect. m=corresponding material



Considering these *in vitro* findings, we decided to determine the osteogenic capacity of osteostatin loaded in these mesoporous materials *in vivo*. To this end, we developed a bone regeneration model by causing a cavity defect in rabbit femur. At 4 weeks from the defect, both the SBA-15 and the C8-SBA-15 promoted osteointegration, with the presence of connective and osteoid tissue, in accordance with earlier studies with other ceramic materials<sup>35</sup>. This effect was greater in the case of both materials with the adsorbed osteostatin, as the presence of neoformed trabeculae in the environs of the biomaterial and a lower thickness of the fibrous capsule indicated, above all after 8 weeks. The lack of inflammatory response with these biomaterials, as the significant absence of cells stained for RAM11 (macrophages) and TRAP indicated, as a consequence of their stability (without apparent degradation), constitutes an advantage of these types of biomaterial<sup>36</sup>. However, a sustained inflammation associated with the degradation of materials such as  $\beta$ -TCP (ultraporous tricalcium phosphate) or DCaS (dense calcium sulphate) may compromise bone regeneration in bone defects as a consequence of an decoupling of bone regeneration and resorption<sup>36</sup>. In addition, although the immunostaining for VEGF was faint, it was possible to observe a revascularisation in the defect zone. In this vein,

Table 1. Structural parameters of the bone at different distances from each of the biomaterials implanted, with or without PTHrP (107-111) at two and four weeks from the defect cavity being produced in the rabbit femur

4 weeks		SBA-15		SBA-15+ PTHrP (107-111)		C8-SBA-15		C8-SBA-15+ PTHrP (107-111)	
Distance (µm)	BV/TV (%)	Tb.Pf (mm <sup>-1</sup> )	BV/TV (%)	Tb.Pf (mm <sup>-1</sup> )	BV/TV (%)	Tb.Pf (mm <sup>-1</sup> )	BV/TV (%)	Tb.Pf (mm <sup>-1</sup> )	
109	0.50±0.09	60.82±1.14	27.74±1.04*	28.01±0.35*	2.01±0.98	35.62±1.46	26.75±1.10*	0.59±0.10*	
327	3.82±0.35	28.27±2.22	14.48±0.90*	14.35±1.45	4.03±1.20	28.37±0.23	17.60±0.53*	8.01±0.42*	
8 weeks		SBA-15		SBA-15+ PTHrP (107-111)		C8-SBA-15		C8-SBA-15+ PTHrP (107-111)	
Distance (µm)	BV/TV (%)	Tb.Pf (mm <sup>-1</sup> )	BV/TV (%)	Tb.Pf (mm <sup>-1</sup> )	BV/TV (%)	Tb.Pf (mm <sup>-1</sup> )	BV/TV (%)	Tb.Pf (mm <sup>-1</sup> )	
109	13.65±0.22	17.42±0.89	24.24±0.95*	19.92±0.72	1.95±0.59	35.24±0.92	2.86±0.44	8.75±0.21*	
327	25.75±0.58	14.68±0.11	44.08±1.22*	6.25±0.15*	1.13±0.12	44.96±1.41	23.29±0.82*	4.11±0.33*	

BV/TV (%) percentage of bone volume; Tb.Pf. trabecular bone pattern factor. The data correspond to a representative rabbit from each group. \*p<0.05 vs material without corresponding load.

two recent studies by our group have demonstrated that the systemic administration of PTHrP (107-111) stimulates angiogenesis and the VEGF system in the tibia in regeneration in osteopenic diabetic mice, or in those treated with glucocorticoids<sup>18,19</sup>. The properties of PTH and the N-terminal fragment of PTHrP as anabolic agents when administered systemically in humans and in animal models with osteoporosis and/or bone fracture are known<sup>37</sup>. Specifically, studies in which PTHrP (1-36) or a synthetic analogue of PTHrP (RS-66271) were used demonstrated an increase in bone mineral density (BMD) in the vertebral spine in postmenopausal women<sup>38</sup> as well as in cortical and trabecular bone in osteopenic rats<sup>39</sup>. Also, RS-66271 administered systemically has been shown to be efficacious in increasing bone repair in rabbits treated with glucocorticoids (osteopenic), increasing BMD and biomechanical parameters and normalising those histological changes associated with bone loss<sup>23</sup>. On the other hand, different local bone factors, such as IL-1/6, IGF-1 (growth factor similar to type 1 insulin), TGF-β (transforming growth factor) or the bone morphogenetic proteins (BMPs) have been proposed as possible agents for the promotion of bone repair<sup>40</sup>, although there are few studies of the effects of these factors incorporated in to a material in this context.

The local release of growth factors in bone defects, as represented by the model used in this work, has been demonstrated to be efficacious and advantageous compared with their exogenous administration. Thus, a study in rats with a seg-

mentary defect in the femur and implanted with degradable matrices containing plasmid DNA of BMP4 and/or the fragment 1-34 of PTH increased (to the greatest extent when the matrix contained both factors) bone neoformation in this defect<sup>41</sup>. Some authors have studied the interaction between endogenous PTHrP and IGF-1 as regulators for bone repair following a fracture in rats<sup>42</sup>. In this model, in initiating the formation of cartilaginous callus IGF-1 appears to increase chondrogenesis, while PTHrP would regulate the rate of differentiation of chondrocytes and, following endochondral ossification, the two factors appear to act in a coordinated way to increase osteogenesis through autocrine/paracrine actions. PTHrP, whose expression increases in the preosteoblast cells by means of its N-terminal fragment, could stimulate the differentiation and synthesis of collagen in these cells by means of IGF1<sup>42</sup>. The results obtained in this cavity defect model support the hypothesis that the C-terminal fragment of PTHrP exerts local anabolic effects to promote bone repair, possibly independently of IGF-1, this being based on previous *in vitro* data<sup>13</sup>. The data exposed highlight the importance of osteostatin as an anabolic factor released locally in the environs of the implanted materials, as the histology and the µCT analysis show.

The existence of a certain variability in the results obtained may be due to the following reasons: it was attempted to reduce the number of rabbits used in accordance with the ethics guide for the protection of animals, carrying out multi-interventions in both femurs. Also, the reproduci-

bility of the cavity defect, as well as the histological analysis (difficult to cut in paraffin with the material) and of the  $\mu$ CT, had their limitations due to what has already been described above.

In view of the results given, PTHrP (107-111) loaded into the C8-SBA-15 material exerts a higher osteogenic effect in comparison with the non-functionalised material. It is possible that this greater effect is due to the peptide remaining adsorbed in the ceramic, whose residual concentrations have been shown to be sufficient to stimulate the proliferation of the osteoblast cells *in vitro*, in comparison with SBA-15 in which the peptide is released more rapidly<sup>14</sup>.

## Conclusions

In conclusion, the capacity of the ceramic biomaterials SBA-15 and C8-SBA-15 to support the local release of PTHrP (107-111) favouring the regeneration of bone following a cavity defect in the femur of rabbit is proven. In addition, the functionalisation of SBA-15 with C8 groups and their subsequent loading with PTHrP (107-111) allows the obtaining of an ideal material for the promotion of bone regeneration in this way. The findings here presented support the possible utilisation of these materials loaded with osteostatin as an alternative therapy for the repair and regeneration of bone.

**Acknowledgements:** This study was carried out thanks to assistance from the Carlos III Institute of Health (Instituto de Salud Carlos III) (PI050117, PI080922, and RETICEF RD06/0013/1002), the Spanish Ministry of Education and Health (Ministerio de Educación y Ciencia de España) (SAF2005-05254), Médica Mutua Madrileña Research Foundation (Fundación de Investigación Médica Mutua Madrileña), the Interministerial Committee for Science and Technology (Comisión Interministerial de Ciencia y Tecnología) (CICYT, Spain) (MAT2008-736) and the Autonomous Community of Madrid (Comunidad Autónoma de Madrid) (S2009/MAT-1472). DL is a post-doctoral researcher associated with the project of the Community of Madrid (Comunidad de Madrid) (S2009/MAT-1472).

## Bibliography

1. Philbrick WM, Wysolmersky JJ, Galbraith S, Holt E, Orloff JJ, Yang KH, et al. Defining the

Figure 3. Representative images (analysed by  $\mu$ CT) of the bone neoformation at different distances for each of the biomaterials studied, with or without PTHrP (107-111) at 4 weeks from making the cavity defect in the rabbit femur

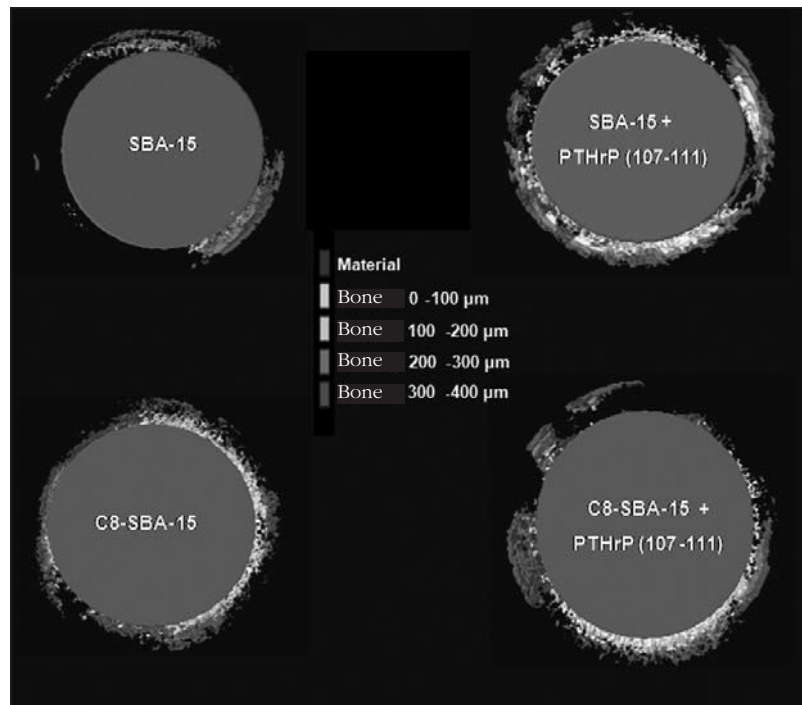


Figure 4. Representative images of the Masson staining in rabbit femurs with implants of biomaterials SBA-15 (A) or C8-SBA-15 (C) loaded or not loaded (B and D respectively) with PTHrP (107-111) at 8 weeks after the cavity defect. m=corresponding material

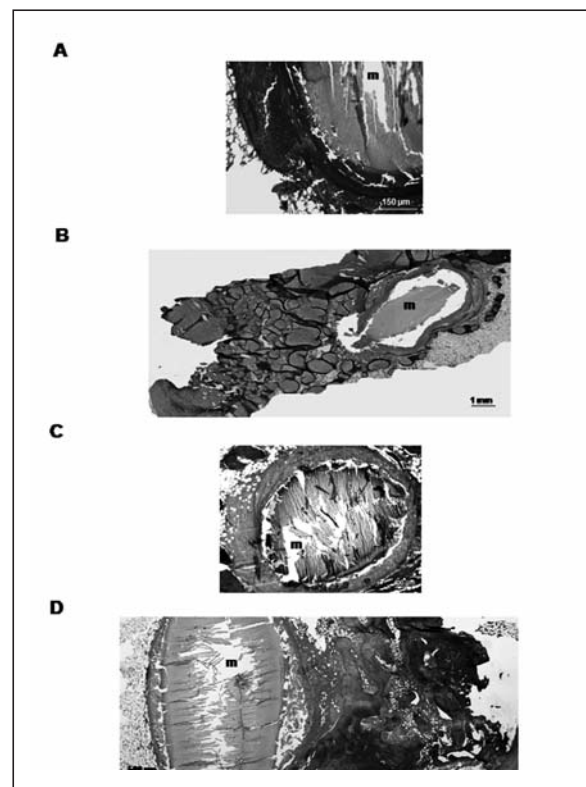


Figure 5. Representative images (analysed by  $\mu$ CT) of the bone neoformation at different distances for each of the biomaterials studied, with or without PTHrP (107-111) at 8 weeks from making the cavity defect in the rabbit femur

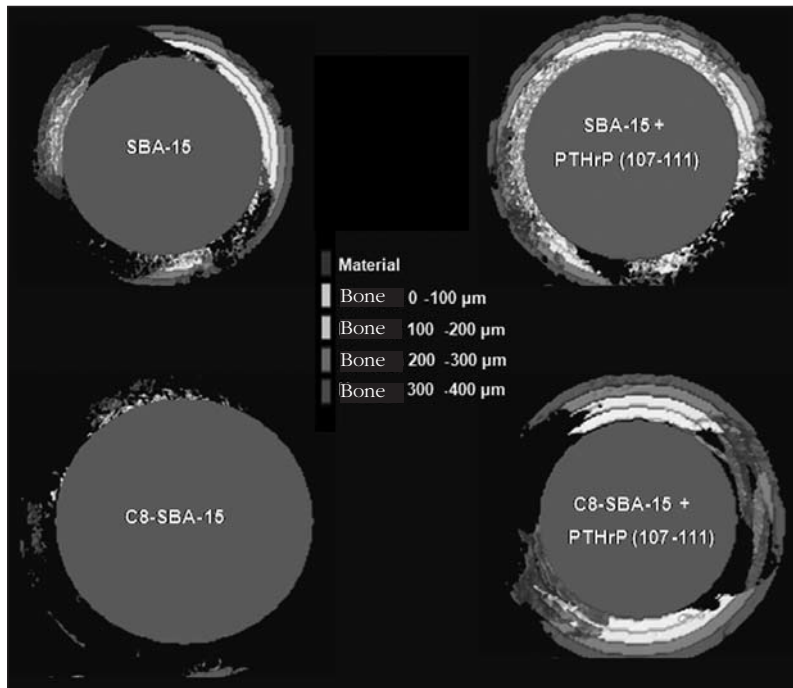
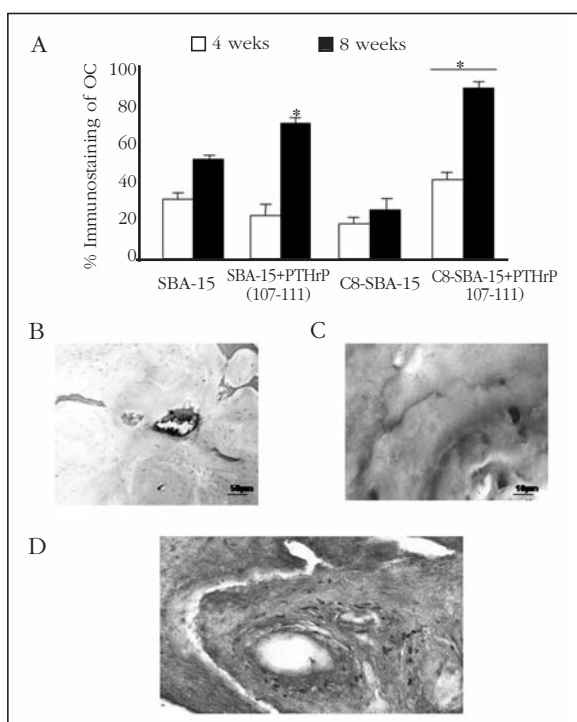


Figure 6. Immunostaining for osteocalcin (OC) in the vicinity of the biomaterials studied loaded or not with PTHrP (107-111), at 4 and 8 weeks from the production of the cavity defect in rabbit femur. The results are means  $\pm$  SEM of 3 rabbits per each experimental group. \* $p < 0.05$  vs. material without corresponding load. Representative images of immunostaining of TRAP (B), RAM11 (C) and VEGF (D) in the vicinity of the material



roles of parathyroid hormone-related protein in normal physiology. *Physiol Rev* 1996;76:127-73.

2. Martin TJ, Moseley JM, Williams DE. Parathyroid hormone-related protein: hormone and cytokine. *J Endocrinol* 1997;154:23-37.

3. de Castro LF, Lozano D, Portal-Núñez S, Maycas M, De la Fuente M, Caeiro JR, Esbrit P. Comparison of the skeletal effects induced by daily administration of PTHrP (1-36) and PTHrP (107-139) to ovariectomized mice. *J Cell Physiol* 2012;227:1752-60.

4. Horwitz MJ, Tedesco MB, Gundberg C, García-Ocana A, Stewart AF. Short-term, high-dose parathyroid hormone-related protein as a skeletal anabolic agent for the treatment of postmenopausal osteoporosis. *J Clin Endocrinol Metab* 2003;88:569-75.

5. Stewart AF, Cain RL, Burr DB, Jacob D, Turner CH, Hock JM. Six-month daily administration

of parathyroid hormone and parathyroid hormone-related protein peptides to adult ovariectomized rats markedly enhances bone mass and biomechanical properties: a comparison of human parathyroid hormone 1-34, parathyroid hormone-related protein 1-36, and SDZ-parathyroid hormone 893. *J Bone Miner Res* 2000;15:1517-25.

6. Stewart AF. PTHrP (1-36) as a skeletal anabolic agent for the treatment of osteoporosis. *Bone* 1996;19:303-6.

7. Fenton AJ, Kemp BE, Hammonds RG, Mitchelhill D, Moseley JM, Martin TJ, et al. A potent inhibitor of osteoclastic bone resorption within a highly conserved peptapeptide region of PTHrP (107-111). *Endocrinology* 1991;129:3424-6.

8. Fenton AJ, Kemp BE, Kent GN, Moseley JM, Zheng MH, Rowe DJ, et al. A carboxyl-terminal peptide from the parathyroid hormone-related protein inhibits bone resorption by osteoclasts. *Endocrinology* 1991;129:1762-8.

9. Fenton AJ, Martin TJ, Nicholson GC. Long-term culture of disaggregated rat osteoclasts: inhibition of bone resorption and reduction of osteoclast-like cell number by calcitonin and PTHrP[107-139]. *J Cell Physiol* 1993;155:1-7.

10. Cornish J, Callon KE, Nicholson GC, Reid IR. Parathyroid hormone-related protein-(107-139) inhibits bone resorption in vivo. *Endocrinology* 1997;138:1299-304.

11. Boileau G, Tenenhouse HS, Desgroseillers L, Crine P. Characterization of PHEX endopeptidase catalytic activity: identification of parathy-

- roid-hormone-related peptide 107-139 as a substrate and osteocalcin, PPI and phosphate as inhibitors. *Biochem J* 2001;355:707-13.
12. Cornish J, Callon KE, Lin C, Xiao C, Moseley JM, Reid IR. Stimulation of osteoblast proliferation by C-terminal fragments of parathyroid hormone-related protein. *J Bone Miner Res* 1999;14:915-22.
  13. De Gortázar AR, Alonso V, Álvarez-Arroyo MV, Esbrit P. Transient exposure to PTHrP (107-139) exerts anabolic effects through vascular endothelial growth factor receptor 2 in human osteoblastic cells in vitro. *Calcif Tissue Int* 2006;79:360-9.
  14. Lozano D, Manzano M, Doadrio JC, Salinas AJ, Vallet-Regí M, Gómez-Barrena E, et al. Osteostatin-loaded bioceramics stimulate osteoblastic growth and differentiation. *Acta Biomater* 2010;6:797-803.
  15. Valín A, Guillén C, Esbrit P. C-terminal parathyroid hormone-related protein (PTHrP) (107-139) stimulates intracellular Ca<sup>2+</sup> through a receptor different from the type 1 PTH/PTHrP receptor in osteoblastic osteosarcoma UMR 106 cells. *Endocrinology* 2001;142:2752-9.
  16. Guillén C, Martínez P, de Gortázar AR, Martínez ME, Esbrit P. Both N- and C-terminal domains of parathyroid hormone-related protein increase interleukin-6 by NF- $\kappa$ B activation in osteoblastic cells. *J Biol Chem* 2002;277:28109-17.
  17. Alonso V, de Gortázar AR, Ardura JA, Andrade-Zapata I, Álvarez-Arroyo MV, Esbrit P. Parathyroid hormone-related protein (107-139) increases human osteoblastic cell survival by activation of vascular endothelial growth factor receptor-2. *J Cell Physiol* 2008;217:717-27.
  18. Fernández de Castro L, Lozano D, Dapía S, Portal-Núñez S, Caeiro JR, Gómez-Barrena E, et al. Role of the N- and C-terminal fragments of parathyroid hormone-related protein as putative therapies to improve bone regeneration under high glucocorticoid treatment. *Tissue Eng Part A* 2010;16:1157-68.
  19. Lozano D, Fernández-de-Castro L, Portal-Núñez S, López-Herradón A, Dapía S, Gómez-Barrena E, et al. The C-terminal fragment of parathyroid hormone-related peptide promotes bone formation in diabetic mice with low turnover osteopaenia. *Br J Pharmacol* 2011;162:1424-38.
  20. Deschaseaux F, Sensébé L, Heymann D. Mechanisms of bone repair and regeneration. *Trends Mol Med* 2009;15:417-29.
  21. Walsh WR, Sherman P, Howlett CR, Sonnabend DH, Ehrlich MG. Fracture healing in a rat osteopenia model. *Clin Orthop Relat Res* 1997;342:218-27.
  22. Andreassen TT, Ejersted C, Oxlund H. Intermittent parathyroid hormone (1-34) treatment increases callus formation and mechanical strength of healing rat fractures. *J Bone Miner Res* 1999;14:960-8.
  23. Bostrom MP, Gamradt SC, Asnis P, Vickery BH, Hill E, Avnur Z, et al. Parathyroid hormone-related protein analog RS-66271 is an effective therapy for impaired bone healing in rabbits on corticosteroid therapy. *Bone* 200;26:437-42.
  24. Vallet-Regí M, Balas F, Arcos D. Mesoporous materials for drug delivery. *Angew Chem Int Ed* 2007;46:7548-58.
  25. Vallet-Regí M. Evolution of bioceramics within the field of biomaterials. *Comptes Rendus Chimie* 2010;13:174-85.
  26. Manzano M, Colilla M, Vallet-Regí M. Drug delivery from ordered mesoporous matrices. *Expert Opin Drug Deliv* 2009;6:1383-400.
  27. Zhao D, Feng J, Huo Q, Melosh N, Fredrickson GH, Chmelka BF, et al. Triblock copolymer syntheses of mesoporous silica with periodic 50 to 300 angstrom pores. *Science* 1998;279:548-52.
  28. Vallet-Regí M. Revisiting ceramics for medical applications. *Dalton Trans* 2006;28:5211-20.
  29. Balas F, Manzano M, Colilla M, Vallet-Regí M. L-Trp adsorption into silica mesoporous materials to promote bone formation. *Acta Biomater* 2008;4:514-22.
  30. Zhao D, Huo Q, Fena J, Chmelka BF, Stucky GD. Non ionic triblock and star diblock copolymer and oligomeric surfactant synthesis of highly ordered, hydrothermally stable, mesoporous silica structures. *J Am Chem Soc* 1998;120:6024-36.
  31. Zambonin G, Camerino C, Greco G, Patella V, Moretti B, Grano M. Hydroxyapatite coated with hepatocyte growth factor (HGF) stimulates human osteoblasts in vitro. *J Bone Joint Surg* 2000;82:457-60.
  32. Zambonin G, Grano M, Greco G, Oreffo ROC, Triffitt JT. Hydroxyapatite coated with insulin-like growth factor 1 (IGF1) stimulates human osteoblast activity in vitro. *Acta Orthop Scand* 1999;70:217-20.
  33. Hoemann CD, Sun J, McKee MD, Chevrier A, Rossomacha E, Rivard GE, et al. Chitosan-glycerol phosphate/blood implants elicit hyaline cartilage repair integrated with porous subchondral bone in microdrilled rabbit defects. *Osteoarthritis Cartilage* 2007;15:78-89.
  34. Feldkamp LA, Davis IC, Kress JW. Practical cone-beam algorithm. *J Opt Soc Am A* 1984;1:612-9.
  35. Kosmulski M. PH-dependent surface charging and points of zero charge. II. Update. *J Colloid Interface Sci* 2004;275:214-24.
  36. Hing KA, Wilson LF, Buckland T. Comparative performance of three ceramic bone graft substitutes. *Spine J* 2007;7:475-90.
  37. Lozano D, de Castro LF, Dapía S, Andrade-Zapata I, Manzarbeitia F, Álvarez-Arroyo MV, et al. Role of parathyroid hormone-related protein in the decreased osteoblast function in diabetes-related osteopenia. *Endocrinology* 2009;150:2027-35.
  38. Horwitz MJ, Tedesco MB, Gundberg C, García-Ocana A, Stewart AF. Short-term, high-dose parathyroid hormone-related protein as a skeletal anabolic agent for the treatment of postmenopausal osteoporosis. *J Clin Endocrinol Metab* 2003;88:569-75.

39. Vickery BH, Avnur Z, Cheng Y, Chiou SS, Leaffer D, Caulfield JP, et al. RS-66271, a C-terminally substituted analog of human parathyroid hormone-related protein (1-34), increases trabecular and cortical bone in ovariectomized, osteopenic rats. *J Bone Miner Res* 1996;11:1943-51.
40. Linkhart TA, Mohan S, Baylink DJ. Growth factors for bone growth and repair: IGF, TGF beta and BMP. *Bone* 1996;19:1S-12S.
41. Fang J, Zhu YY, Smiley E, Bonadio J, Rouleau JP, Goldstein SA, et al. Stimulation of new bone formation by direct transfer of osteogenic plasmid genes. *Proc Natl Acad Sci U S A* 1996;93:5753-8.
42. Okazaki K, Jingushi S, Ikenoue T, Urabe K, Sakai H, Iwamoto Y. Expression of parathyroid hormone-related peptide and insulin-like growth factor I during rat fracture healing. *J Orthop Res* 2003;21:511-20.

**Guede D<sup>1,2</sup>, Pereiro I<sup>3</sup>, Solla E<sup>3</sup>, Serra J<sup>3</sup>, López-Peña M<sup>4</sup>, Muñoz F<sup>4</sup>, González-Cantalapiedra A<sup>4</sup>, Caeiro JR<sup>2,5</sup>, González P<sup>3</sup>**

1 Trabeculae - Empresa de Base Tecnológica, S.L. - Ourense

2 Red Temática de Investigación en Envejecimiento y Fragilidad (RETICEF) - Instituto de Salud Carlos III - Ministerio de Economía y Competitividad - Madrid

3 Grupo de Nuevos Materiales - Departamento de Física Aplicada - Universidad de Vigo - Pontevedra

4 Departamento de Ciencias Clínicas Veterinarias - Facultad de Veterinaria - Universidad de Santiago de Compostela - Lugo

5 Servicio de Cirugía Ortopédica y Traumatología - Complejo Hospitalario Universitario de Santiago de Compostela - A Coruña

## Osteointegration and biocompatibility *in vivo* of bio-inspired silicon carbide ceramics in an experimental model in rabbits

Correspondence: David Guede - Trabeculae, S.L. Parque Tecnológico de Galicia - Edificio "Tecnópole I"  
Local 22 - 32900 San Cibrao das Viñas - Ourense (Spain)  
e-mail: dguede@trabeculae.com

Date of receipt: 27/07/2012

Date of acceptance: 02/11/2012

*Working FEIOMM scholarship to attend the 33rd Congress of the ASBMR (San Diego, 2011)*

### Summary

**Background:** The new generation of materials for implants should imitate the hierarchical structures found in nature. Bio-inspired silicon carbide ceramic (bioSiC) is a ceramic produced from wood, which has a similar structure to bone, with a unique property of interconnected porosity, which allows the internal growth of tissue and favours angiogenesis.

**Objectives:** To evaluate the biocompatibility and osteointegration of bioSiC in femoral bone defects in an experimental model in rabbits.

**Material and methods:** 36 cylinders of bioSiC were obtained through pyrolysis of sapelli wood and infiltration with molten silicon of the resulting carbon preform. Eighteen cylinders were coated with Si-HA by pulsed laser deposition. The cylinders were implanted in femoral condyles of rabbits which were sacrificed at 1, 4 or 12 weeks. The samples were analysed histologically using an optical microscope and computerised microtomography to assess bone growth.

**Results:** The bioSiC implants showed good osteointegration, there being both outward growth (ongrowth) and inward growth (ingrowth). At 4 weeks from implantation the integration was almost complete, with no difference from that seen at 12 weeks. The coating did not improve the value of any parameter with respect to the non-coated implants.

**Conclusions:** BioSiC ceramics produced from porous wood have good osteointegration and their interconnected porosity is colonised by bone tissue. In addition, they do not require the bioactivity of a coating to improve the apposition of neoformed bone. BioSiC stands as a material to be taken into account in biomedical applications.

**Key words:** *silicon carbide, bone substitutes, osteointegration, histological techniques, X-ray computerised microtomography.*

## Introduction

Traditionally, bone defects have been treated by autologous (coming from the patient themselves), allogenic (coming from another individual of the same species) or xenogenic (with bone obtained from another species) tissue transplants, or even by implanting substitute materials. The autografts, although they have a shown a high percentage rate of success, are limited by the quantity of tissue which may be extracted and by the morbidity of the extraction site<sup>1</sup>. On their part, allografts and xenografts (which are much less often used) may cause immune reactions and transmit pathogens to the patient. With regard to synthetic bone substitutes, all of these enjoy a number of advantages over bone grafts, such as their unlimited availability or their ease of sterilisation. However, in spite of their great variety, the main problem with all of them is their limited ability to provide mechanical support in the affected zone<sup>2</sup>. Current demands on the engineering of tissues for the regeneration of bone tissue raises new challenges in material sciences and biomedical engineering. Arising from this is a trend towards technology based on biomimetics for the development of new biomaterials, which are inspired by models and biostructures which nature offers, and which have been perfected and optimised through the evolutionary process.

Bioinspired ceramic materials, based on natural precursors such as wood, plants or algae, bring together a number of the characteristics required of this new generation of biomaterials: good biomechanical properties, lightness, toughness, and with a hierarchical and interconnected porous structure which assimilates with bone tissue to encourage the growth of this tissue in its interior, as well as angiogenesis, which means to say the osteointegration of the material into the host tissue<sup>3</sup>. Bioinspired silicon carbide ceramics (BioSiC) bring together all the biomechanical requirements sufficient for their use as bone substitutes. These ceramics may be made from a variety natural structures<sup>4,5</sup>. The technological fabrication process is based on the ceramicisation of the natural precursors, obtaining as a final result a piece of silicon carbide with an interconnected porosity which maintains its hierarchical structure in terms of the size and distribution of the pores of the original material.

Mechanical trials indicate that the properties of these materials may be made to measure by the selection of the appropriate vegetal precursor from which they are made, depending on the characteristics of the type of bone which is being attempted to be repaired, and by modifying the experimental conditions of the fabrication process. Thus, it is notable that, as with bone, bioSiC has anisotropic mechanical properties, with values which compare favourably with those of bone. For example, the bioSiC obtained using sapelli wood (*Entandrophragma cylindricum*) has values of resistance to longitudinal compression (the growth axis of the tree) of  $210\pm 20$  to  $1.160\pm 100$

MPa, and a radial direction from  $120\pm 10$  to  $430\pm 50$  MPa as a function of the quantity of Si with which it has been infiltrated<sup>6,7</sup>. The resistance to compression of specimens of human cortical bone vary between 167 and 215 MPa<sup>8</sup>.

The biocompatibility of a material refers to its capacity to function as a substrate which will support appropriate cell activity, facilitating systems of cellular and mechanical signalling, with the aim of optimising the regeneration of tissues without provoking undesirable reactions in the host<sup>9</sup>. The aim of this study was to confirm the capacity for osteointegration of bioSiC ceramics in an animal model of a bone defect in rabbit, confirming its biocompatibility *in vivo* through a comparison of implants with bioactive coating and those without.

## Material and methods

### Fabrication of bioinspired SiC

The process of making the bioinspired ceramics consists of two basic phases. The first is the process of pyrolysis, in which the natural precursor, dried and lyophilised is subject to a high temperature in inert conditions. The sample was heated at a controlled rate of  $2^\circ\text{C}/\text{min}$  up to  $600\text{--}800^\circ\text{C}$ . This temperature was maintained for 1 hour and then the sample was slowly cooled to room temperature. The resulting material is a carbonaceous structure/matrix which retains all the biostructural details of the vascular system of the original precursor.

The second phase consists of a process of infiltration, in which the carbon structure/matrix is covered with silicon powder and exposed to a high temperature in a controllable oven in vacuum conditions. A temperature of  $1,550^\circ\text{C}$  is reached, at a rate of  $5\text{--}10^\circ\text{C}/\text{min}$ , kept at the maximum temperature for 30 min, followed by a controlled cooling at  $20^\circ\text{C}/\text{min}$ , producing a piece of silicon carbide. For this study 36 cylinders of bioSiC derived from sapelli wood were made, of which 18 were coated with Si-HA (7.5 at.%) by means of pulsed laser deposit (PLD). The process of coating the Si-HA was carried out with an excimer laser (193 nm, 175 mJ and 10Hz) using a synthetic pellet of hydroxyapatite (HA) and silicon powder (7.5 at.% of Si). The deposit was performed in an atmosphere of water vapour (0.45 mbar) keeping the substrate at  $460^\circ\text{C}$  during the growth of the coating.

### Animal model

To investigate the *in vivo* biocompatibility of the material an experimental model of a bone defect in a rabbit femur was designed. The cylinders of bioSiC were implanted in the lateral condyles of the femurs of 18 New Zealand rabbits. This was carried out by means of lateral longitudinal distal approach in the thighs of both extremities, and with a drill an orifice was made in the distal epiphysis of the femur in which was implanted, selected at random, a cylinder of bioSiC with no coating, or a cylinder of bioSiC with a bioactive coating of Si-HA. The animals were sacrificed

using an intravenous administration of sodium phenobarbital at 1, 4 and 12 weeks following the implant and samples were obtained, which were fixed in formol buffered at 10%. With this approach, 6 experimental groups were obtained (n=6), the first three with non-coated implants for the three periods of study, and the last three with coated implants. All the experiments were carried out in conformance with the Law 14/2007 and the Royal Decree 1201/2005, and following the directives of the UNE-EN rules 30993-3:1994 and ISO 10993-2:2006.

### Histological analysis

The samples were processed for study using the techniques of embedding in methacrylate described by Donath<sup>10</sup> following the stages of fixing, dehydration, infiltration, inclusion and polymerisation. Subsequently, longitudinal sections were made in the condyle of the femur approximately 30  $\mu\text{m}$  thick, which were stained using the Lévai-Laczkó stain.

Once prepared, the samples were examined with a binocular microscope and the fraction of the total pore area occupied by bone, the quantity of neoformed bone in the periphery of the implant and the percentage of the surface of the implant in contact with bone were estimated<sup>11</sup>. The later calibration was carried out using the Microimage computer application.

### Analysis using micro-CT

The formation of bone around the implant was also analysed using computerised microtomography (micro-CT). The samples were scanned using a SkyScan 1172 high resolution X-ray microtomograph (Bruker micro CT NV, Kontich, Belgium) with the intensity of the X-ray source at 60 kV and 167  $\mu\text{A}$ . A nominal resolution of 7.9  $\mu\text{m}$  was used and an Al filter of 1mm thickness used to obtain a restricted longitudinal wave interval. The rotation step was 0.2° with a total rotation of 360° and a frame averaging value (images per step) of three. The images obtained were reconstructed using the modified Feldkamp algorithm<sup>12</sup> and analyses using the commercial application CTAnalyser (Bruker micro CT NV, Kontich, Belgium). For this, a volume of interest of 160  $\mu\text{m}$  thickness from the surface of the implant was selected, in which was determined the bone volume fraction (BV/TV). In addition, the surface area of the intersection of the bone with the implant with reference to the total surface area of the implant (i.S/TS) was calculated.

### Statistical analysis

The data gathered in this study were entered into a text database which was subsequently exported to the statistics software package SPSS 18.0 (IBM, Armonk, NY, USA) for their later statistical analysis. Then the descriptive analysis was made of the variables in the study. The descriptive statistics for the numerical variables were expressed as mean  $\pm$  standard deviation. The com-

parative statistical study of all the numerical results obtained for the different groups of the study was carried out using the Mann-Whitney U test due to the fact that the variables did not exceed the normality criteria applied. The relationship between the results obtained by histology and micro-CT were studied using Pearson's correlation.

The level of statistical significance was established at  $p < 0.05$  for all the variables analysed.

### Results

The *in vitro* biocompatibility of the bioSiC ceramics was demonstrated using a culture of the human osteoblast cell line MG-63 in an earlier study<sup>7</sup>. To investigate the biocompatibility *in vivo* of these bioceramics an experimental model in rabbit femur was used. The histological slides obtained for the samples after the implantation were examined using optical microscope and computerised microtomography.

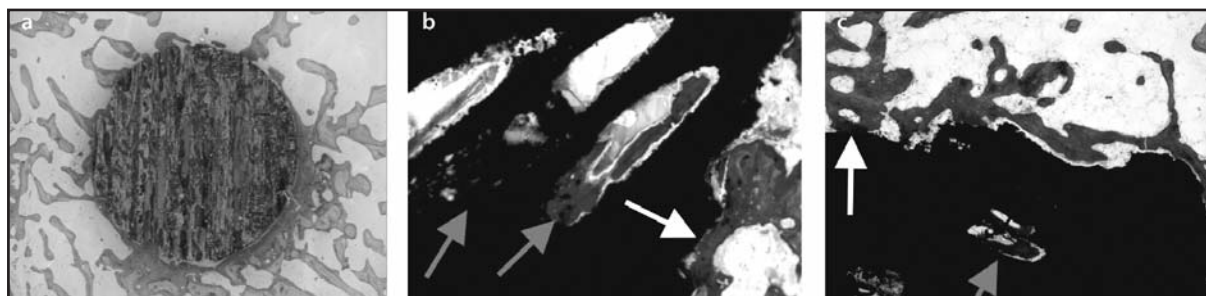
Through the histological analysis it is possible to observe the growth of neoformed bone on the surface of the implants, with no signs of inflammation or appearance of fibrous tissue in the region of the samples. It is notable that the neoformed bone penetrates the pores of the implant. At higher magnifications of the microscope we can confirm this colonisation, as well as the bone's contact with the implant, which is a key feature (Figure 1).

In the implants without coating, at the first week after implantation it is observed that 10.38% of the area of the pores have been colonised by new bone, a percentage which increases to 37.52% at 4 weeks ( $p = 0.017$ ). In the area selected in the periphery of the implant the neoformed bone after the first week occupied 21.25%, while at 4 weeks it was 31.30% ( $p = 0.030$ ). At 12 weeks no differences were observed in any variable with respect to the samples at 4 weeks (Figure 2).

In the analysis with micro-CT, the region of interest selected for the analysis of bone growth was 160  $\mu\text{m}$  from the surface of the implant. After the first week from the positioning of the bioSiC implants, the BV/TV of the region analysed was 11.49%, which means that of the volume analysed around the implant, this percentage was occupied by bone. At 4 weeks, the BV/TV increased to 45.36% ( $p = 0.030$  vs 1st week). The value at 12 weeks showed no significant difference to that at 4 weeks. Similarly, the i.S/TS, which represents the percentage of the surface of the implant in contact with bone, increases up to the fourth week, after which its value appears to stabilise, leaving approximately half the surface of the implant in contact with neoformed bone. Again, no differences were found between the groups at 4 and 12 weeks (Figures 2 and 3).

The relationship between the results obtained using the two techniques was studied using Pearson's correlation. The BV/TV calculated by micro-CT had a positive correlation with the percentage of neoformed bone in the periphery determined by histology ( $r = 0.588$ ,  $p < 0.001$ ); there

Figure 1. Histological images of a cylinder of bioSiC 12 weeks after implantation: a) the growth of bone around and inside the pores of the implant, with no fibrous tissue separating bone and implant observed; b) and c) the colonisation of the pores by bone tissue at higher magnification and its contact with the biomorphic ceramic are observed



was a similar relationship between the microtomographic intersection surface (i.S/TS) and the percentage of bone contact determined histologically ( $r=0.677$ ,  $p<0.001$ ) (Figure 4).

## Discussion

Nature offers a great variety of species with highly diverse levels of porosity, which means that we must select the original precursor most appropriate to the bone structure which we wish to replicate. Notable among their common characteristics is the disposition of having a hierarchical porous structure which is replicated in the bioinspired ceramics.

In the case of sapelli, we see a combination of microcanals with a diameter of between 80 and 100  $\mu\text{m}$ , which have an impact on the promotion of vascularisation, and the transport of nutrients and waste products. Also observed are micropores of around 4  $\mu\text{m}$  which participate in the formation of the capillaries<sup>7</sup>. Notable also is the presence of pores on the nanometric scale which play an interesting role in matters relating to molecular diffusion for nutrition and signalling. The interconnection of the pores provide a channel for cellular migration and allow the formation of blood vessels; and the roughness of the material contributes to increasing the surface area, favouring the adsorption of proteins and ion interchange<sup>3</sup>.

From the values obtained both through histological analysis and microstructural analysis with micro-CT it can be deduced that osteointegration is complete after 4 weeks. None of the parameters analysed by either of the techniques show significant differences between the samples at 4 and 12 weeks, either in the samples with the coating or those without. The samples in which a coating of Si-HA has been applied had no significant differences from the bioSiC samples without a coating for any of the variables analysed. From this fact it is deduced that the bioinspired SiC ceramics do not need the addition of a coating in order to be biocompatible, and that the coating does not improve its contact with bone.

The bioinspired ceramics of silicon carbide have, therefore, great potential as new materials

for biomedical applications. The feasibility of producing strong lightweight ceramic devices with interconnected porosity suitable for use as bone substitutes has been demonstrated. The *in vivo* trials of bioSiC implants indicate that the pores of this material are colonised by bone tissue and support its mineralisation. They also confirm that they have a good apposition for neoformed bone and good osteointegration in a relatively short time after implantation.

## Bibliography

1. Salgado AJ, Coutinho OP, Reis RL. Bone tissue engineering: State of the art and future trends. *Macromol Biosci* 2004;4:743-65.
2. Vicario Espinosa C. Los aloinjertos óseos en Cirugía Ortopédica y Traumatología (1). *Patología Aparato Locomot* 2004;2:214-32.
3. Ratner BD, Hoffman AS, Schoen FJ, Lemons JE (eds). *Biomaterials Science: Introduction to Materials in Medicine*, 2nd Edition. London: Elsevier Academic Press; 2004.
4. Martínez-Fernández J, Varela-Feria FM, Singh M. High temperature compressive mechanical behavior of biomorphic silicon carbide ceramics. *Scr Mater* 2000;43:813-8.
5. De Arellano-López AR, Martínez-Fernández J, González P, Domínguez C, Fernández-Quero V, Singh M. BiomorphiC SiC: A new engineering ceramic material. *Int J Appl Ceram Technol* 2004;1:56-67.
6. Kardashev BK, Burenkov YuA, Smirnov BI, de Arellano-López AR, Martínez-Fernández J, Varela-Feria FM. Elasticity and inelasticity of biomorphic silicon carbide ceramics. *Phys Solid State* 2004;46:1873-7.
7. González P, Borrajo JP, Serra J, Chiussi S, León B, Martínez-Fernández J, et al. A new generation of bio-derived ceramic materials for medical applications. *J Biomed Mater Res A* 2009;88:807-13.
8. An YH. Mechanical properties of bone. In: An YH, Draughn RA (eds.). *Mechanical testing of bone and the bone-implant interface*. Boca Raton, Florida, (USA): CRC Press; 2000.

Figure 2. Graphic representation of the results of the structural variables obtained through micro-CT: a) bone volume fraction (BV/TV), b) surface percentage of the intersection of the bone and implant (i.S/TS); and through histology: c) percentage of the bone area formed on the periphery of the implant, d) percentage of the surface of the implant in contact with bone and e) percentage of bone area formed in the interior of the implant in relation to the total pore area

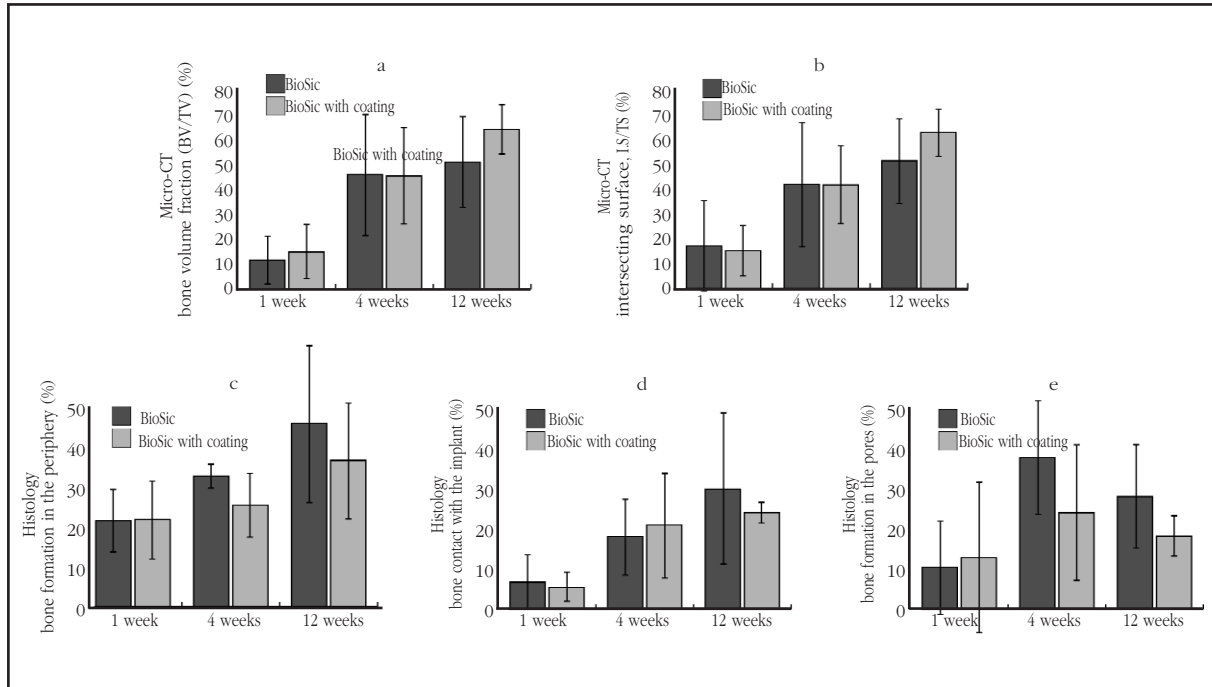


Figure 3. Three dimensional models of the ceramic bioSiC at 1, 4 and 12 weeks (a, b) and bioactive coating bioSiC with Si-HA (d, e and f). Ceramic cylinders are shown in dark gray the new bone at the periphery of the implant in light gray

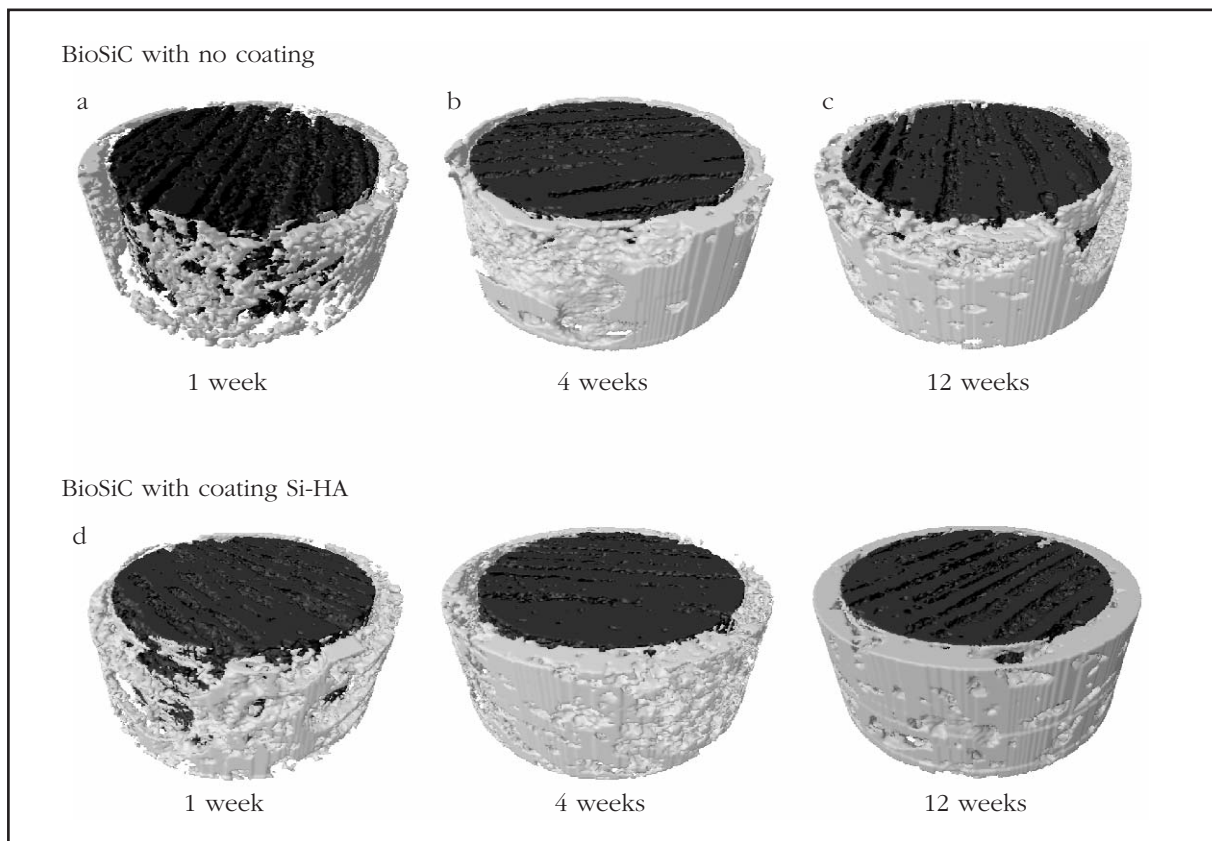
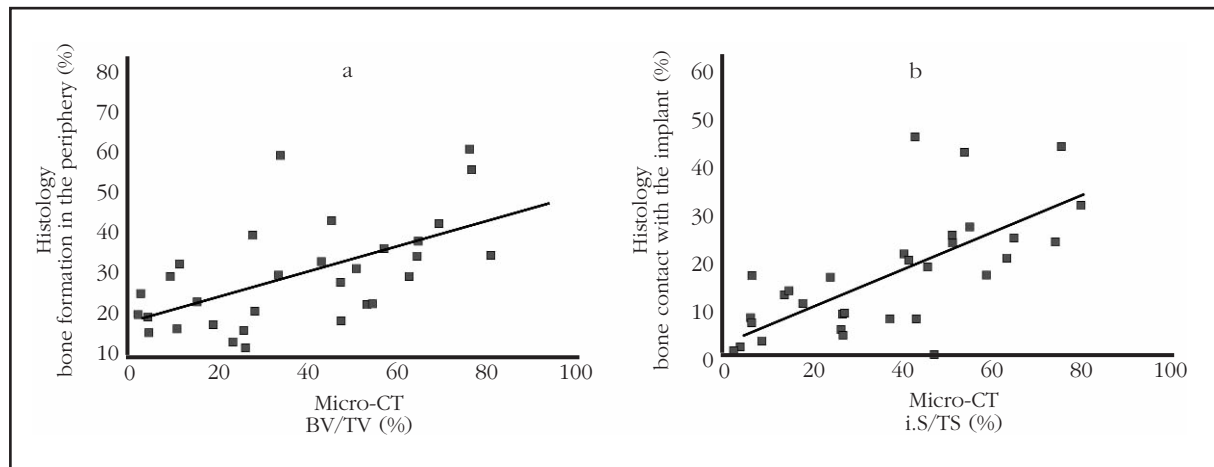


Figure 4. Dispersion diagram with the parametric data obtained using micro-CT and histology: a) the microtomographic bone volume fraction compared with the formation on the periphery determined by histology, both variables which quantify the bone formed around the implants of bioSiC; b) the percentage of the surface of the implant in contact with bone, measured by micro-CT and histology



9. Williams D. Revisiting the definition of biocompatibility. *Med Device Technol* 2003;14:10-3.
10. Donath K. Preparation of histologic sections by the cutting-grinding technique for hard tissue and other material not suitable to be sectioned by routine methods. Norderstedt: Institute for Pathologie, University of Hamburg; Exakt-Kulzer-Publication; 1995.
11. Tonino AJ, Thèrin M, Doyle C. Hydroxyapatite-coated femoral stems: Histology and histomorphometry around five components retrieved at post mortem. *J Bone Joint Surg Br* 1999;81:148-54.
12. Feldkamp LA, Davis LC, Kress JW. Practical cone-beam algorithm. *J Opt Soc Am A* 1984;1:612-9.

**Delgado-Calle J<sup>1</sup>, Sañudo C<sup>1</sup>, Sumillera M<sup>2</sup>, Garcés CM<sup>2</sup>, Riancho JA<sup>1</sup>**

<sup>1</sup> Departamento de Medicina Interna - H.U. Marqués de Valdecilla - IFIMAV - Universidad de Cantabria - Santander

<sup>2</sup> Departamento de Cirugía Ortopédica y Traumatología - H.U. Marqués de Valdecilla - Santander

## Expression of RANKL and OPG in primary osteoblasts

Correspondence: José A. Riancho - Departamento de Medicina Interna - Hospital U.M. Valdecilla - IFIMAV - Universidad de Cantabria - Av. Marqués de Valdecilla, s/n - 39008 Santander (Spain)  
e-mail: rianchoj@unican.es

Date of receipt: 20/06/2012

Date of acceptance: 19/11/2012

### Summary

**Objective:** Osteoblasts are specialized cells responsible for bone formation. Furthermore, these cells modulate osteoclast formation and maturation, mainly by the production of RANKL and OPG. We previously reported that the bone tissue of osteoporotic patients showed increased RANKL expression and RANKL/OPG ratio when compared to osteoarthritic patients. Thus we decided to explore whether this aberrant expression may be related to an abnormal expression of these genes by osteoblasts. The aim of this study was to explore the transcriptional levels of these factors in primary osteoblasts.

**Methods:** Primary human osteoblasts (hOBs) were obtained by the primary explant technique from bone tissue of patients undergoing hip replacement surgery for hip fractures (n=28) or osteoarthritis (n=26). Patients with secondary osteoporosis, fractures due to high-energy trauma or secondary osteoarthritis were excluded. RANKL and OPG gene expression was explored by real time quantitative PCR.

**Results:** No statistical differences in RANKL and OPG gene expression were found along the *in vitro* mineralization of hOBs. Interestingly, OPG transcriptional levels were markedly higher than RANKL levels. However, no differences in the transcriptional levels of RANKL and OPG were observed between both groups.

**Conclusions:** Overall, our data confirm that osteoblasts produce RANKL and OPG. However, our results suggest that the gene expression differences found in the osteoporotic and osteoarthritic bone tissue are not explained by the intrinsic characteristics of osteoblasts.

**Key words:** osteoclastogenesis, bone remodeling, osteoporosis, osteoarthritis.

## Introduction

Bone is a specialised form of supporting tissue formed by different cell types and mineralised materials on which they confer marked rigidity and resistance, at the same time as allowing a certain degree of elasticity. Due to this peculiar composition, bone tissue is also an important reservoir of calcium and other inorganic ions, and participates actively in the maintenance of calcium homeostasis. Each bone is sculpted by means of a complicated process called modelling<sup>1</sup>. In addition, bone tissue is renewed constantly by a process known as remodelling<sup>2</sup>. Remodelling plays an essential role in the homeostasis of calcium, as well as preserving the solidity of the bone by substituting old bone for new.

Differently from modelling, bone remodelling requires the coordinated action of the osteoclasts, cells which are in charge of reabsorbing bone, and osteoclasts, bone-forming cells. Basically, the process of remodelling may be divided into four phases<sup>3,4</sup>. The first phase, known as activation, involves the process of starting remodelling by the activation of the osteoclasts in a specific region of the bone by means of the attraction of osteoclast precursors and the induction of their differentiation into mature osteoclasts. In the second stage, resorption, the osteoclasts are fixed in a bone matrix creating a resorption cavity. The resorption phase ends with the apoptosis of the osteoclasts. Together with the osteoclast apoptosis signals responsible for the recruitment of the osteoblasts to the resorption cavities are produced (the proliferation phase). This coupling between the action of the osteoclasts and the osteoblasts is sequential in such a way that the processes of bone resorption and formation do not coexist either in time or space. Indeed, this is critical in order for there to be a proper process of remodelling. Finally, during the last stage, known as the formation stage, the osteoblasts synthesise the non-mineralised organic matrix, and are subsequently responsible for their mineralisation.

In spite of the fact that all not all the details of the molecular mechanisms of these processes are known, some of them have been successfully identified. The RANKL-RANK signalling system, critical for the initiation of osteoclastogenesis, is perhaps the most important molecular mechanism for the differentiation of the osteoclasts<sup>5</sup>. The receptor activator of nuclear factor  $\kappa$ B ligand (RANKL) is a protein produced by various types of cells, among which the osteoblasts are one of the principal sources in bone tissue<sup>6</sup>. This protein bonds to the receptor activator of nuclear factor  $\kappa$ B (RANK), present in the membranes of the osteoclast precursors, inducing their differentiation through the ultimate activation of transcription factor NFATc-1, which is responsible for the modulation of the expression of the genes necessary for the formation of an osteoclast which is mature and prepared for bone resorption<sup>7</sup>. On the other hand, the osteoblasts are also capable of producing osteoprotegerin (OPG), another protein which acts as

a soluble receptor for RANKL, thus blocking the possible interaction between RANKL and its receptor RANK<sup>8</sup>. In fact the RANKL/OPG quotient determines in great measure the rate of osteoclastogenesis. Directly related to this, in an earlier work we observed that the gene expression of RANKL and the RANKL/OPG quotient in bone tissue are significantly higher in patients with osteoporotic fractures than in patients with arthrosis, suggesting that the patients with osteoporosis may have a greater activation of osteoclastogenesis, and, as a consequence, an imbalance in bone remodelling, which provokes a loss of bone mass and a greater probability of suffering fractures<sup>9</sup>. In spite of the fact that data from other authors confirm these results<sup>10,11</sup>, for the moment what it is that provokes these differences in the production of RANKL and OPG is not known.

Given their capacity to produce RANKL and OPG the osteoblasts are not only crucial for bone formation, but they are also essential for the initiation of osteoclastogenesis and a correct coupling of resorption-formation. Therefore, the aim of this work was to study the changes in expression of RANKL and OPG in primary osteoblasts during the process of mineralisation *in vitro* and to compare the levels of transcription in osteoblasts taken from osteoporotic and arthrotic patients.

## Materials and methods

### Cell cultures

Bone tissue samples were obtained from the femoral head during substitutive arthroplasties. The study was approved by the regional committee for ethics in clinical research and all the samples were taken after obtaining informed consent. The primary osteoblast samples were obtained using the explants technique<sup>12</sup>, using trabecular bone tissue from the central part of the femoral head, avoiding the fractured areas and subchondral regions. The osteoblasts were cultivated in DMEM, complemented with 10% foetal bovine serum and antibiotics, and kept in an incubator at 37° C under 5% CO<sub>2</sub> and with a relative humidity of above 90%.

For the mineralisation experiments the cells were plated at a density of 40,000 cells/cm<sup>2</sup>. Once the cells had arrived at a state of confluence osteogenic medium (DMEM, complemented with 10% foetal bovine serum, antibiotics, 50  $\mu$ m ascorbic acid and 10mM of  $\beta$ -glycerophosphate) was added. The progress of calcification was studied by staining with Alizarin Red S<sup>13</sup>. For the analysis of the expression of RANKL and OPG in arthrotic and osteoporotic patients cultures of primary osteoblasts with a confluence of 80% (passes 1-2) from patients subject to the insertion of a hip prosthesis due to fracture or arthrosis were used. The patients were selected using the determining criteria for the diagnosis of osteoporosis and arthrosis, in the former, the presence on fractures and in the latter the presence of serious arthrosis. Excluded from the study were those patients with secondary osteoporosis, with fractures due to high energy trauma or with secondary arthrosis.

### Gene expression

RNA was extracted from semiconfluent primary osteoblasts using TRIzol, following the instructions of the manufacturer (Invitrogen). For the synthesis of cDNA 1 µg of RNA was used and the instructions of the maker of the Superscript III First Strand kit (Invitrogen) were followed. During the culture of the cells in osteogenic medium RNA was extracted consecutively every 7 days.

The gene expression for RANKL and OPG was quantified using quantitative PCR (RT-qPCR) with TaqMan probes following the manufacturer's instruction (Applied Biosystems). To avoid inter-experimental variability samples from the both groups were included in each of the analyses carried out. The TaqMan probes used were: TNFSF11 (isoform I, RANKL: Hs00243519\_m1 and TNFRSF11B (OPG): Hs00900360\_m1. For each gene the relative expression was calculated using as a reference the gene of the TATA box binding protein (TBP), expressed consecutively in the cells. The expression was calculated using the 2- $\Delta$ Ct method,  $\Delta$ Ct being the difference between the umbral cycle (Ct) of the gene of interest and TBP.

### Statistical analysis

For the comparison of the expression of RANKL and OPG during the process of osteogenic expression the Student's t-test (two tails), was used. The statistical significance of the differences between the patients with osteoporosis and arthrosis were studied with the Mann-Whitney test (two tails). The value  $p=0.05$  was fixed as the limit of statistical significance. The data were analysed with the GraphPad Prism statistical programme, version 5.01.

## Results

### Study of the expression of RANKL and OPG during the process of mineralisation *in vitro*

The primary osteoblast cultures in osteogenic conditions showed a progressive mineralisation, evidenced by staining with Alizarin Red S (Figure 1A). In parallel we studied the expression of RANKL and OPG during the process (Figure 1B). The expression of RANKL showed a tendency to increase with the advance in calcification, becoming notable after three weeks in culture, although it did not become statistically significant. On the other hand, we detected no differences in transcriptional levels of OPG (Figure 1C). It should be noted that the gene expression of OPG was much higher than that of RANKL during the whole process. As a consequence, the values of the RANKL/OPG quotient were noticeably low, although again we observed a non-significant tendency to increase with the time in culture (Figure 1D).

### Study of the expression of RANKL and OPG in primary osteoblasts from patients with fracture and with arthrosis

Table 1 summarises the characteristics of those patients from whom the samples were obtained. We found no significant differences in the gene

expression of RANKL, OPG or in the RANKL/OPG quotient, between the two groups of osteoblasts analysed (Table 2). As with the mineralization medium cultures in both groups OPG expression was notably higher than that of RANKL. On the other hand we analysed the results by stratifying the samples by age. In spite of the fact that no significant differences were found, the osteoblasts obtained from the arthrotic patients aged between 81 and 90 years showed a clear tendency to express more OPG. Similarly, the RANKL/OPG quotient was lower in the osteoblast cultures from patients with arthrosis (Table 3).

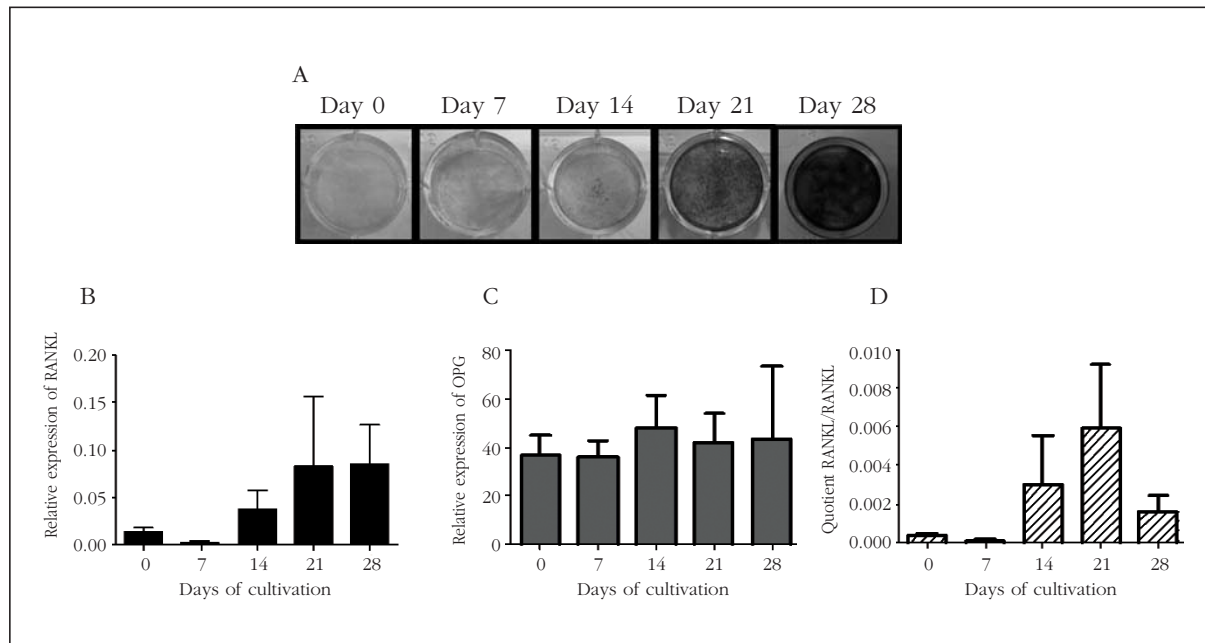
Finally, we analysed the data separating the samples by sex. No differences were found between women and men when the two groups of osteoblasts were compared. Similarly, no differences were found between women and men in the same group (Table 4).

## Discussion

Since the discovery of the RANKL-OPG-RANK signalling system there have been many studies designed to understand the mechanisms which regulate it. Studies with "knock out" mice have shown that the absence of these genes is directly related to changes in bone mass<sup>14</sup>. Therefore, this system has become a valuable therapeutic target for the treatment of prevalent skeletal diseases such as osteoporosis. In fact, the antibodies against RANKL have been shown to reduce the number of fractures in postmenopausal osteoporotic patients<sup>15</sup>. Therefore, it seems clear that this is one of the signalling mechanisms critical for bone homeostasis, capable of tipping the balance towards greater or lesser resorption as a function of the relationship between the production of RANKL and OPG.

At the moment it is not known precisely which are the mechanisms which trigger the commencement of bone remodelling, but it is thought that it is the osteocytes which are responsible for signalling the location and for recruiting the osteoclast precursors to the region, supposedly through a process of chemoattraction<sup>16,17</sup>. The production of RANKL by the osteoblasts, and, as has recently been published, by the osteocytes<sup>18</sup>, induces the maturation of the osteoclast precursors and starts the resorption. However, osteoblast and osteoclasts do not coexist in time or space. On the one hand, it is known that the osteoclasts undergo apoptosis and disappear. On the other, our data from *in vitro* mineralisation using primary osteoblasts suggest that during bone formation there is a greater gene expression of OPG than RANKL. This, theoretically, would reduce the possibility of an interaction between RANKL and RANK, thus preventing a possible activation of osteoclastogenesis during bone formation. Curiously, the expression of RANKL and OPG does not appear to be modified significantly during the process of mineralisation. However, there is observed a slight tendency to an increase in the expression of RANKL in later days, in those cases in which the

Figure 1. Gene expression of RANKL and OPG in a process of mineralisation *in vitro* in primary osteoblasts. A) Every 7 days, the mineral deposition was evaluated using Alizarin Rd S. B) The expression of RANKL showed a non-significant tendency to increase with time. C) The expression of OPG was constant throughout the process of mineralisation *in vitro*. D) The RANKL/OPG quotient increases non-significantly in the final days of the process. Presented in the figures are the mean and standard deviation of the values of relative expression obtained from the process of mineralisation with 4 independent samples of primary osteoblasts



mineralisation was more patent. This slight increase in the expression of RANKL is accompanied by a slight increase in the RANKL/OPG quotient.

Osteoporosis and arthrosis are two skeletal diseases characterised by having opposing bone mass values<sup>19</sup>. While the osteoporotic patients showed a reduction in bone mass compared with healthy subjects, those with arthrosis tended to have a higher bone mass. Given the impact that RANKL and OPG have on bone homeostasis, it may be expected that the difference in the production of these proteins may explain, at least in part, the differences in bone mass between these patients. Thus, our group has recently shown that the production of RANKL, and as a consequence, the RANKL/OPG quotient, is increased in the bone tissue of osteoporotic patients<sup>9</sup>. Other authors have reported similar results, which suggests that this really is pattern of expression characteristic of osteoporotic patients. In an attempt to find an explanation for this deregulation of RANKL expression, we studied whether there were differences in the methylation of the promoter regions for this gene in bone tissue of osteoporotic and arthrotic patients, but this was not the case. However, it should be taken into account that bone tissue is formed by different cell types, a number of which are capable of producing RANKL and OPG. Therefore we decided to study the expression of these genes selectively in primary osteoblasts from osteoporotic and arthrotic patients. As observed in primary osteoblast mine-

ralization, in both osteoporotic and arthrotic patients the values of OPG expression were higher than those of RANKL. In the overall analysis of the results we found no significant differences in the expression of RANKL or OPG between the two groups studied. These results are in line with earlier observations carried out by other groups<sup>20-22</sup>. Nor did we find any differences when we analysed expression by sex or age. However, we did find a clear tendency to a higher expression of OPG in arthrotic patients aged between 81 and 90 years, and as a consequence, those same patients showed a lower RANKL/OPG quotient. Together, these results suggest that the differences observed in bone tissue were not due to the osteoblasts of the osteoporotic or arthrotic patients being intrinsically different in terms of the expression of these genes. It is possible that the differences at the level of tissue may be explained by differential production on the part of other types of cell, such as the osteocytes or cells of the immune system. In concordance with the this the RANKL/OPG quotient found in the primary osteoblast cultures was much lower than that found in the bone tissue<sup>9</sup>, which means that other cells different from the osteoblasts contribute to the production of RANKL in the bone tissue. Similarly, it has recently been suggested that the osteocytes are the principal source of RANKL in the bone, at least in mice<sup>18</sup>.

It is therefore possible to speculate that the differences found may be due to a differential production of RANKL specifically in this type of cell.

Table 1. Distribution of sex and age of the samples collected for the analysis of the expression of RANKL and OPG

	N			Age		
	Total	Women	Men	Total	Women	Men
<b>FRX</b>	28	23	5	81±6	82±6	79±5
<b>ART</b>	26	9	17	75±6	73±9	76±4
<b>Value p</b>				0.003	0.20	0.02

Table 2. Values for gene expression (mean and standard deviation) for the RANKL and OPG gene in primary osteoblasts

	OPG	RANKL	RANKL/OPG
<b>FRX</b>	25.52±4.06	0.024±0.013	0.001±0.0006
<b>ART</b>	45.86±19.67	0.042±0.023	0.042±0.039
<b>Value p</b>	0.57	0.50	0.81

Table 3. Analysis stratified by age for the gene expression of RANKL and OPG in primary osteoblasts (mean and standard deviation)

	Age		OPG		RANKL		RANKL/OPG	
	70-80	81-90	70-80	81-90	70-80	81-90	70-80	81-90
<b>FRX</b>	75±1	85±3	24.9±4.7	26.92±6.36	0.02±0.01	0.02±0.02	0.002±0.001	0.0006±0.0002
<b>ART</b>	73±1	82±2	25.0±8.2	133±93.76	0.03±0.02	0.05±0.05	0.049±0.048	0.0001±0.0001
<b>Value p</b>	0.21	0.14	0.69	0.09	0.57	0.23	0.18	0.052

Table 4. Analysis stratified by sex for the gene expression of RANKL and OPG in primary osteoblasts (mean and standard deviation)

	OPG		RANKL		RANKL/OPG	
	♀	♂	♀	♂	♀	♂
<b>FRX</b>	26.73±0.01	23.02±7.05	0.028±0.012	0.008±0.004	0.0013±0.0007	0.0003±0.0001
<b>ART</b>	96.77±53.88	18.96±5.02	0.096±0.066	0.014±0.006	0.1131±0.1129	0.0017±0.0011
<b>Value p</b>	0.35	0.47	0.93	0.31	0.40	0.64

In fact, it would not be surprising that the osteocytes in osteoporotic patients had an abnormal production of RANKL, since we have already observed in earlier works a change in the expression of various genes involved in bone metabolism<sup>23</sup>. Similarly, the osteoblastic lining cells, considered to be inactive osteoblasts, may be implicated in the differences in the expression of RANKL in bone tissue, since our studies indicate that the pattern of methylation of the promoter of the RANKL gene allows these cells to be capable of expressing both RANKL and OPG<sup>9</sup>.

On the other hand, we should not forget that, when working with primary cells, these are isolated in their usual surroundings, the bone microen-

vironment, without their being stimulated by factors capable of modulating the production of RANKL and OPG, positively or negatively. Various molecules, such as the parathyroid hormone or the estrogens, among many others, can alter the expression of these genes and, therefore, may be responsible for the deregulation reported in osteoporotic patients. Finally, our analysis has focused exclusively on gene expression, without evaluating the quantity of protein present. Similarly, earlier works have shown that, in spite of finding no differences at a transcriptional level, the synthesis of OPG is increased in osteoblasts taken from osteoporotic patients<sup>20,22</sup>. The causes of this de-synchronisation between transcriptional and

protein levels are currently unknown. One may speculate about a possible deregulation of the expression of certain miRNAs being capable of influencing the process of translating messenger RNA or changes in post-translation marks which affect the stability or half-life of the protein. So it would be interesting to carry out studies to confirm whether the differences observed at a transcriptional level also occur at the level of the proteins, as well as fathoming those post-transcriptional and post-translational mechanisms which influence the quantity of protein produced.

Taken together, our data suggest that the differences in the production of RANKL and OPG found in bone tissue between osteoporotic and arthrosic patients are not due to the intrinsic characteristics of the osteoblasts in these patients, but must have their origin in other skeletal cells, or be the consequence of the complex cellular and molecular interactions which take place in the bone microenvironment. New studies will be needed which focus on other types of cells to indentify the mechanisms which underlie the deregulation of the expression of RANKL in osteoporotic bone.

**Funding:** The work was funded with a AMGEN S.A. (AMGEN-SEIOMM 2009) grant. Jesús Delgado-Calle holds a pre-doctoral grant from IFIMAV. The authors declare that they have no conflict of interest.

### Bibliography

1. Teti, A. Bone development: Overview of bone cells and signaling. *Curr Osteoporos Rep* 2011;9:264-73.
2. Hadjidakis DJ, Androulakis II. Bone remodeling. *Ann N Y Acad Sci* 2006;1092:385-96.
3. Raggatt IJ, Partridge NC. Cellular and molecular mechanisms of bone remodeling. *J Biol Chem* 2010;285:25103-8.
4. Sims NA, Gooi JH. Bone remodeling: Multiple cellular interactions required for coupling of bone formation and resorption. *Semin Cell Dev Biol* 2008;19:444-51.
5. Boyce BF, Xing L. Biology of RANK, RANKL, and osteoprotegerin. *Arthritis Res Ther* 2007;9(Suppl1):S1.
6. Yasuda H, Shima N, Nakagawa N, Yamaguchi K, Kinosaki M, Mochizuki S, et al. Osteoclast differentiation factor is a ligand for osteoprotegerin/osteoclastogenesis-inhibitory factor and is identical to TRANCE/RANKL. *Proc Natl Acad Sci USA* 1998;95:3597-602.
7. Kearns AE, Khosla S, Kostenuik PJ. Receptor activator of nuclear factor kappaB ligand and osteoprotegerin regulation of bone remodeling in health and disease. *Endocr Rev* 2008;29:155-92.
8. Simonet WS, Lacey DL, Dunstan CR, Kelley M, Chang MS, Lüthy R, et al. Osteoprotegerin: a novel secreted protein involved in the regulation of bone density. *Cell* 1997;89:309-19.
9. Delgado-Calle J, Sañudo C, Fernández AF, García-Renedo R, Fraga MF, Riancho JA. Role of DNA methylation in the regulation of the RANKL-OPG system in human bone. *Epigenetics* 2012;7:83-91.
10. Logar DB, Komadina R, Prezelj J, Ostaneč B, Trost Z, Marc J. Expression of bone resorption genes in osteoarthritis and in osteoporosis. *J Bone Miner Metab* 2007;25:219-25.
11. D'Amelio P, Roato I, D'Amico L, Veneziano L, Suman E, Sassi F, et al. Bone and bone marrow pro-osteoclastogenic cytokines are up-regulated in osteoporosis fragility fractures. *Osteoporos Int* 2011;22:2869-77.
12. Velasco J, Zarrabeitia MT, Prieto JR, Perez-Castrillon JL, Perez-Aguilar MD, Perez-Núñez MI, et al. Wnt pathway genes in osteoporosis and osteoarthritis: differential expression and genetic association study. *Osteoporos Int* 2010;21:109-18.
13. Delgado-Calle J, Sañudo C, Sánchez-Verde L, García-Renedo RJ, Arozamena J, Riancho JA. Epigenetic regulation of alkaline phosphatase in human cells of the osteoblastic lineage. *Bone* 2011;49:830-8.
14. Khosla S. Minireview: the OPG/RANKL/RANK system. *Endocrinology* 2001;142:5050-5.
15. Bone HG, Bolognese MA, Yuen CK, Kendler DL, Wang H, Liu Y, et al. Effects of denosumab on bone mineral density and bone turnover in postmenopausal women. *J Clin Endocrinol Metab* 2008;93:2149-57.
16. Rochefort GY, Pallu S, Benhamou CL. Osteocyte: the unrecognized side of bone tissue. *Osteoporos Int* 2010;21:1457-69.
17. Bonewald LF. The amazing osteocyte. *J Bone Miner Res* 2011;26:229-38.
18. Nakashima T, Hayashi M, Fukunaga T, Kurata K, Oh-Hora M, Feng JQ, et al. Evidence for osteocyte regulation of bone homeostasis through RANKL expression. *Nat Med* 2011;17:1231-4.
19. Dequeker J, Aerssens J, Luyten FP. Osteoarthritis and osteoporosis: clinical and research evidence of inverse relationship. *Aging Clin Exp Res* 2003;15:426-39.
20. Giner M, Rios MJ, Montoya MJ, Vázquez MA, Miranda C, Pérez-Cano R. Alendronate and raloxifene affect the osteoprotegerin/RANKL system in human osteoblast primary cultures from patients with osteoporosis and osteoarthritis. *Eur J Pharmacol* 2011;650:682-7.
21. Giner M, Montoya MJ, Vázquez MA, Rios MJ, Moruno R, Miranda MJ, et al. Modifying RANKL/OPG mRNA expression in differentiating and growing human primary osteoblasts. *Horm Metab Res* 2008;40:869-74.
22. Giner M, Rios MA, Montoya MA, Vázquez MA, Naji L, Pérez-Cano R. RANKL/OPG in primary cultures of osteoblasts from post-menopausal women. Differences between osteoporotic hip fractures and osteoarthritis. *J Steroid Biochem Mol Biol* 2009;113:46-51.
23. Delgado-Calle J, Arozamena J, García-Renedo R, García-Ibarbia C, Pascual-Carra MA, González-Macías J, et al. Osteocyte deficiency in hip fractures. *Calcif Tissue Int* 2011;89:327-34.

**Civantos Modino S<sup>1</sup>, Navea Aguilera C<sup>1</sup>, Pavón de Paz I<sup>1</sup>, Almodovar Ruiz F<sup>2</sup>, Elviro Peña MR<sup>1</sup>**

<sup>1</sup> Servicio Endocrinología y Nutrición - Hospital Universitario de Getafe - Madrid

<sup>2</sup> Servicio Endocrinología y Nutrición - Fundación Hospital Alcorcón - Madrid

## Bone metastases and cord compression debut as follicular thyroid carcinoma

Correspondence: Soralla Civantos Modino - Carretera de Toledo Km 12,5 - 28995 Getafe - Madrid (Spain)  
e-mail: zulemaciv@hotmail.com

Date of receipt: 11/03/2012

Date of acceptance: 03/09/2012

### Summary

In thyroid carcinoma, distant metastases are infrequent (10-15% of the follicles). The most common sites are the lungs, bones (appearing in the form of lytic lesions), the brain, the liver, the bladder and the skin. The diagnosis of follicular carcinoma through a metastatic complication is exceptional, but it should be considered in the differential diagnosis of a pathological fracture. We present three cases of exceptional occurrence.

**Key words:** *carcinoma, thyroid, metastasis, surgery.*

## Introduction

Differentiated thyroid carcinoma is the most frequent endocrine neoplasia. It is one of the tumours with the highest potential probability of being cured and with a highly favourable prognosis for metastatic disease characterised by a slow progression and a survival rate at 10 years of 34-40%<sup>1,2</sup>.

Distant metastases are infrequent (10-15% of the follicles), but in cases where they occur the most common sites are the lung, bone (as lytic lesions), brain, liver, bladder and skin<sup>3</sup>. The diagnosis of a follicular carcinoma through a complication of its metastasis is an exceptional occurrence, but it should be considered in the differential diagnosis of a pathological fracture<sup>4</sup>. In this study 3 cases are presented of patients with medullar compression due to bone metastasis as a first manifestation of a follicular thyroid carcinoma. We believe that these cases are of general interest due to the unusual nature of the findings and the interdisciplinary management which took place.

### Case 1

A 68 year-old woman who in April 2010 started to experience refractory dorsal pain and paresis with loss of strength in the lower limbs. A simple X-ray identified a collapse of the third dorsal vertebra, and she was admitted to the traumatology service with suspected myeloma vs. metastasis. A magnetic nuclear resonance (MNR) scan showed evidence of an affection of the whole vertebral body and the posterior arch, with an associated mass of soft parts which had entered the neural canal compromising the spinal medulla. Also affected was the neural foramen of the second, third and fourth dorsal vertebrae (Figure 1). The findings suggested tumourous lesions, probably metastatic, while not discounting the possibility of a primary myeloma-type tumour. In a thoracic-abdominal computerized axial tomography (CAT) there was evidence of multiple small nodular lesions in both lungs suggestive of metastatic disease, and which a positron emission tomography (PET)/CAT scan showed to be hypermetabolic. The rest of the examination provided no evidence of significant findings. During the same admission an embolisation of the tumour was tried, without success, and a medullar decompression was effected, with the fusion of the dorsal vertebrae from D1 to D6. The anatomical pathology indicated that what was being dealt with was a follicular thyroid carcinoma of the Hürtle cell variety. Notable antecedents from the anamnesis were a hemithyroidectomy, plus isthmectomy, carried out in 1999 in another hospital due to the presence of a nodule with the result of "oncocytoma", without further data or follow up.

An ultrasound of the thyroid was carried out which showed a normal right hemithyroid. A total thyroidectomy was performed, with no evidence of malignance in the tissue removed, and finally, the patient was treated with an ablative dose of Iodine 131 ( $I_{131}$ ) (200 mCi). The post-dose total body scan (TBS) showed an intense capture in the

metastatic areas shown up on the PET/CAT scan. After twelve months of development the patient continued with follow up and treatment by the traumatology and endocrinology services, with the control of symptoms and signs of disease stable.

### Case 2

A woman of 60 years of age in whom, in a simple X-ray study due to pain in the back and lower limbs over a period of 3-4 months, were found lesions suggestive of metastasis in the left femoral neck, dorsal spine (D1, D2 and D12, with infiltration into the spinal canal), left femoral diaphysis and left greater trochanter. A prophylactic femoral pinning was performed. The histological study showed metastasis of follicular thyroid carcinoma. The patient said that in 1993 a left hemithyroidectomy was carried out in another centre, the reasons for which were not made clear. An ultrasound of the thyroid was carried out without significant findings, and a total thyroidectomy was performed with no evidence of malignancy in the tissue removed. Initial thyroglobulin was 67 ng/ml, with negative antithyroglobulin antibodies. The patient was treated with  $I_{131}$  at a dose of 200 mCi, with evidence of the disease now being stable.

### Case 3

A woman of 71 years of age with progressively worsening lumbalgia and the appearance of paresthesia in the lower limbs in May 2008. An MNR showed lytic lesions in L4 and medullar compression compatible with metastatic lesion, which required a vertebrectomy with fusion from the second lumbar vertebra to the first sacral vertebra (L2-S1). An anatomopathological study suggested metastasis of a primary thyroid tumour. An ultrasound was described as "multimodal goitre with hypoechogenic nodules in the isthmus and left lobe of the thyroid, and adenopathy of 2.7 cm in the left jugular-carotid space, with puncture-aspiration with a fine needle (PAFN) of oncocytic proliferation" (*sic*). After a total thyroidectomy the final diagnosis was follicular thyroid carcinoma of the Hürtle cell variety. After the first ablative dose of  $I_{131}$  (200 mCi) there was a persistent Tg value of 17 ng/ml with negative antithyroglobulin antibodies, for which reason it was decided to administer a second dose of  $I_{131}$  (150 mCi) eight months later. In the control PET there was evidence of newly appearing captures in L4, and right iliac wing and clavicle (Figure 2), for which reason a third dose of 200 mCi was administered (accumulated dose of 550 mCi) six months after the second dose. The post-dose tracking showed intense capture in the areas evidenced in the imaging tests. After fifteen months from the last treatment the data relating to the disease were stable without complications derived from the treatment with  $I_{131}$ .

## Discussion

Differentiated thyroid carcinoma has a good prognosis in general, but the natural development of

the disease in some cases is towards distant dissemination, which carries with it an ominous prognosis, with mortality rates of 65% and 75% at 5 and 10 years respectively. The bone metastases are of the osteolytic type and are difficult to visualise in simple X-rays. Fortunately, the cases of vertebral metastases as a way of diagnosing the disease are very rare, and proof of this is that published cases are scarce<sup>5</sup>.

Faced with a lytic lesion in the spinal column it is necessary to make a differential diagnosis fundamentally between myeloma and metastasis. Among the latter the most frequent primary tumour will be found in the prostate, breast and lung, and less commonly, in the kidney, colon, skin and thyroid.

When bone metastases are suspected a total body scan or a PET/CAT scan should be carried out to locate them. MNR is particularly useful in patients with spinal affection and to characterise the metastases once they have been diagnosed. Carrying out a CAT is also valid.

A biopsy of the lesion is fundamental to identifying the origin of the metastasis, but does not distinguish the follicular or papillary lineage. For this it is essential to investigate the thyroid with ultrasound and PAFN.

Treatment should be with an ablative dose of I131 of between 100 and 200 mCi, to be determined through dosimetry. The dose may be repeated at 6-10 months depending on the development of the disease.

Many studies support the benefit in patients with lytic bone metastasis (more specifically, those originating in breast cancer) of the use of bisphosphonates, especially intravenous zoledronate, since these drugs inhibit osteoclast activity, which means its use has been extended to the treatment of other forms of lytic metastasis, such as those of differentiated thyroid carcinoma<sup>6</sup>.

Radiotherapy is indicated in patients with intense pain without medullar complications or with neurological deficit at the start and slow and incomplete progression, as long as vertebral osteoarticular instability is discounted, a key point for the indication of surgery. In those cases in which the prognosis is bad in the short term, or in which the general situation is contraindicative for surgery, it is the only option.. Embolisation is useful for reducing vascularisation of the metastasis, facilitating later surgery, and reducing the growth of the tumour<sup>8</sup>.

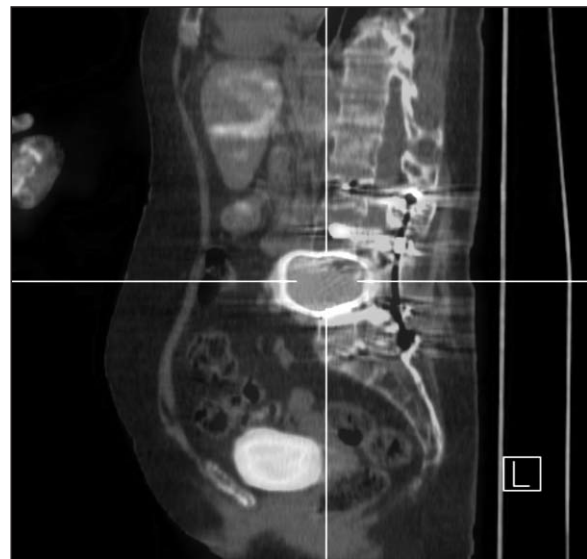
The corticoids are used for their antioedemal effect and are not alone except when the patient's situation does not allow other treatments.

Palliative surgery is indicated when there is a pain of increasing intensity incontrollable by other methods, an acute, complete and rapid onset neurological deficit, or when the destruction of the bone provokes a segmental instability in the spinal column. It may also be used with curative intent if there is only a single metastasis, or they are few in number. It consists of the resection of the tumorous tissue, releasing all the compress-

Figure 1. MNR: Collapse of the body of the 3rd dorsal vertebra and posterior arch with associated mass of soft parts which are entering the neural canal compromising the spinal medulla



Figure 2. PET: pathological capture in the 4th lumbar vertebra



sion on the medullar tissue, and the fixing through vertebral osteosynthesis associated with bone grafts using anterior and/or posterior means of approach, with the intention of fusing the affected segment with those immediately above and below<sup>9,10</sup>.

In conclusion, the diagnosis of a follicular thyroid carcinoma from the discovery of bone metastasis is an exceptional first manifestation, but should be considered within the differential diagnosis of these lesions. Treatment demands interdisciplinary coordination and cooperation for the optimum management of the disease.

### **Bibliography**

1. Schlumberger MJ. Papillary and follicular thyroid carcinoma. *N Eng J Med* 1998;338:297-306.
2. Jemal A, Siegel R, Xu J, Ward E. Cancer Statistics 2010. *Cancer J Clin* 2010;60:277-300.
3. Benbassat C, Mechlis-Frishi S, Hirsch D. Clinicopathological characteristics and long-term outcome in patients with distant metastases from differentiated thyroid cancer. *World J Surg* 2006;30:1088-95.
4. Goldberg H, Stein M, Ben-Itzhak O, Duek D, Ravkin A, Gaitini D. Metastatic spinal cord compression as initial presentation of follicular thyroid carcinoma. *J Surg Oncol* 1998;67:186-9.
5. Scarrow A, Colina JL, Levy E. Thyroid carcinoma with isolated spinal metastasis: case history and review of the literature. *Clin Neurol Neurosurg* 1999;101:245-8.
6. Wexler J. Approach to the thyroid cancer patient with bone metastases. *J Clin Endocrinol Metab* 2011;96:2296-307.
7. Paller CJ, Carducci MA, Philips GK. Management of bone metastases in refractory prostate cancer-role of denosumab. *Clin Interv Aging* 2012;7:363-72.
8. Smit J, Vielvoye G, Goslings B. Embolization for vertebral metastases of follicular thyroid carcinoma. *J Clin Endocrinol Metab* 2000;85:989-94.
9. Carty S, Cooper D, Doherty G, Duh QY, Kloos RT, Mandel SJ, et al. Consensus statement on the terminology and classification of central neck dissection for thyroid cancer. *Thyroid* 2009;19:1153-8.
10. Cooper DS, Doherty GM, Haugen BR, Kloos RT, Lee SL, Mandel SJ, et al. Revised American Thyroid Association Management Guidelines for patients with thyroid nodules and differentiated thyroid cancer. *Thyroid* 2009;19:1167-214.

**Espasa Font L<sup>1</sup>, Supervía A<sup>2</sup>, Del Baño F<sup>2</sup>, I Sarbu M<sup>3</sup>**

1 Servicio de Oncología

2 Servicio de Urgencias

3 Servicio de Reumatología

Hospital Universitario del Mar - Parc de Salut Mar - Barcelona

## Costal right metastasis of prostate adenocarcinoma

Correspondence: August Supervía - Servicio de Urgencias - Hospital Universitario del Mar - Ps. Marítim 25-29 - 08003 Barcelona (Spain)

e-mail: [Asupervia@hospitaldelmar.cat](mailto:Asupervia@hospitaldelmar.cat)

Date of receipt: 20/04/2012

Date of acceptance: 31/08/2012

### Summary

Prostate cancer is one of the most frequent cancers in man and its incidence is growing constantly due to early diagnosis that is now being made by determining levels of PSA in the general health controls. The most common site of metastasis is bone, and these lesions are frequently symptomatic, causing pain, debility, and functional impairment. Skeletal metastases in men with prostate cancer are usually osteoblastic although increases in bone resorption have been consistently demonstrated. A 49 years old man with a recent diagnosis of prostate cancer was admitted to Emergency Department for right thoracic pain. The physical examination showed pain of mechanical characteristics corresponding to the 5th-7th ribs. The chest radiography showed absence of the 6th rib.

**Key words:** *prostate cancer, bone metastases, lysis costal.*

## Introduction

The incidence of prostate cancer has increased in recent years due in part to early detection through the determination of the prostate specific antigen (PSA). Its most common histology is adenocarcinoma (ADC). A number of different factors have been implicated in its aetiology, notable among which is the role of hormones, especially androgenic hormones<sup>1</sup>. A case is presented of a young male affected by ADC of the prostate who sought medical attention due to costal pain and who was diagnosed with tumourous lysis in a costal arch.

## Clinical case

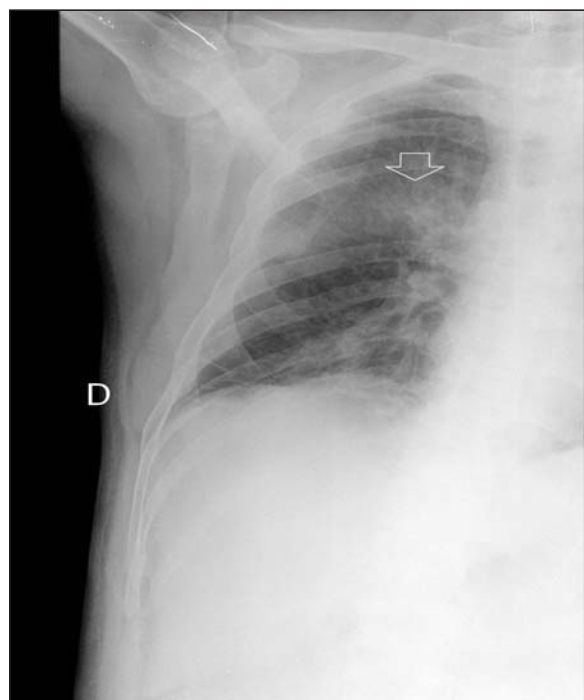
A 49 year-old male with history of cranioencephalic trauma, which was resolved leaving cognitive-behavioural after-effects, and prostate ADC. His first admission was due to persistent lumbosciatica developing over two months, combined with bilateral costal pain with neuropathic characteristics. The diagnosis at discharge was disseminated ADC of the prostate. The complementary examinations showed the existence of multiple bone metastases (M1), as well as the presence of a lump in the right posterior costal arch. The PSA was 13,000 U/l and the alkaline phosphatase (AP) 478 U/l. The bone gammagraphy showed evidence of pathological deposits in the cranium, dorsal vertebrae, right humerus, lesser trochanter, right femoral diaphysis and the left ischial spine, but with no deposits observed in the rib cages to suggest blastic lesions. The biopsy of the costal lump was positive for M1s for ADC of the prostate, which was confirmed with a biopsy of the posterior pros-

tate. During admission the patient showed a disturbance in gait, for which reason a magnetic resonance (MR) scan was carried out of the dorsal spine which showed a medullar compression secondary to epidural M1 in vertebra DVII, with radiotherapy indicated (he received a total dose of 30 Grays). The patient was treated with 50 mg/day of bicalutamide, a quarterly subcutaneous injection of 10.8 mg of gosorelin and zoledronic acid (2 doses i.v. of 4 mg/month diluted in 50 cc of physiological serum) with a satisfactory outcome. Gait rehabilitation was initiated and discharge was 33 days after admission. 23 days following his discharge the patient attended casualty due to the appearance of pain in the right hemithorax. The physical examination showed pain on palpation from the 5th to 7th rib. A blood analysis was carried out which showed calcium levels of 7.14 mg/dl, C-reactive protein of 3.4 mg/dl and AP of 1,297 UI/l. An X-ray of the right rib cage showed an absence of the posterior arch of the 6th rib (Figure 1). The patient was re-admitted to the Oncology Unit where the treatment continued. Now, after four years of follow up, he is in a hormone-resistant phase with the appearance of blastic polytopic bone M1s.

## Discussion

The level of the presence of bone M1s in necropsy studies of patients who have died due to prostatic neoplasia is 90%<sup>2</sup>. The growth of prostate cancer in the bone promotes bone turnover, which produces osteoblast M1s with underlying lytic lesions<sup>3</sup>. The Wnt<sup>3</sup> system has been implicated in the osteoblast activity, while the osteolytic activity may be due to an inhibition of Wnt<sup>3</sup> activity and the participation of the OPG-RANKL system<sup>4</sup>. The percentage of tumorous cells which express OPG and RANKL increases significantly in patients with bone M1s. A combination of both mechanisms could explain the lysis in the rib of this patient. Given the coexistence of the osteoblast and osteolytic mechanisms in the genesis of the M1s, we do not believe that the predominance of one of these mechanisms could have had an influence on the development of the disease in this patient. In terms of treatment, in recent years different drugs which act on bone metabolism have been evaluated for the treatment of neoplastic bone affectations. In the case of prostate cancer, the existence of lytic M1s has resulted in the evaluation of the bisphosphonates. Thus, the simultaneous administration of zoledronic acid combined with hormone treatment in patients with bone M1s at the time of diagnosis may delay the progression of the disease<sup>5</sup>, a fact which may explain the long-term survival of the patient under discussion. However, this effect is not extendible to other bisphosphonates<sup>6</sup>. Another drug which has been shown to be effective is denosumab which has turned out to be even more effective than zoledronic acid<sup>7</sup>. Finally, it should be noted that the appearance of hormone-resistance could be the consequence of the development of the tumour into neuroendocrine

Figure 1. X-ray of the right rib-cage, in which is seen the absence of the posterior arch of the 6th rib (arrow)



prostate ADC, a more aggressive sub-type<sup>8</sup>. In this case, the demonstration of an overexpression of the protein Aurora A kinase may be of use in indicating this possible transformation<sup>8</sup>.

### **Bibliography**

1. Stewart BW and Kleihues P (Eds): World cancer report (International Agency for Reserch on Cancer). World health organization (WHO). World Cancer Report. Lyon: IAR Press;2003.
2. Bubendorf L, Schopfer A, Wagner U, Sauter G, Moch H, Willi N, et al. Metastatic patterns of prostate cancer: An autopsy study of 1,589 patients. *Hum Pathol* 2000;31:578-83.
3. Hall CL, Bafico A, Dai J, Aaronson SA, S  ller ET. Prostate cancer cells promote osteoblastic bone metastases through Wnts. *Cancer Res* 2005;65:7554-60.
4. Brown JM, Corey E, Lee ZD, True LD, Yun TJ, Tondravi M, et al. Osteoprotegerin and RANK ligand expression in prostate cancer. *Urology* 2001;57:611-6.
5. Uemura H, Yanagisawa M, Ikeda I, Fujinami K, Iwasaki A, Noguchi S, et al. Possible anti-tumor activity of initial treatment with zoledronic acid with hormonal therapy for bone-metastatic prostate cancer in multicenter clinical trial. *Int J Clin Oncol* 2012 Apr 11. [Epub ahead of print]. Doi: 10.1007/s10147-012-0406-8.
6. Mackiewicz-Wysocka M, Pankowska M, Wysocki PJ. Progress in the treatment of bone metastases in cancer patients. *Expert Opin Investig Drugs* 2012;21:785-95.
7. Fizazi K, Garducci M, Smith M, Damiao R, Brown J, Karsh L, et al. Denosumab versus zoledronic acid for treatment of bone metastases in men with castration-resistant prostate cancer. *Lancet* 2011;377:813-22.
8. Beltran H, Rickman DS, Park K, Chae SS, Sboner A, MacDonald TY, et al. Molecular characterization of neuroendocrine prostate cancer and identification of new drug targets. *Cancer Discov* 2011;1:487-95.

Ovejero Gómez VJ<sup>1</sup>, Díez Muñiz-Alique M<sup>2</sup>, Díez Lizuáin ML<sup>3</sup>, Pérez Martín A<sup>1</sup>, Azcarretazábal González-Ontaneda T<sup>4</sup>, Ingelmo Setien A<sup>1</sup>

1 Servicio de Cirugía General y Aparato Digestivo

2 Servicio de Endocrinología y Nutrición

3 Servicio de Radiodiagnóstico

4 Servicio de Anatomía Patológica

Hospital Sierrallana de Torrelavega - Cantabria

## Hypercalcemia crisis due to complex parathyroid tumour: a diagnostic and surgical dilemma

Correspondence: Víctor J. Ovejero Gómez - Servicio de Cirugía General y Aparato Digestivo - Hospital Sierrallana de Torrelavega - Barrio de Ganzo, s/n - 39300 - Torrelavega - Cantabria (Spain)  
e-mail: vovejerohcas@msn.com

Date of receipt: 13/06/2012

Date of acceptance: 11/11/2012

### Summary

The clinical manifestation of primary hyperparathyroidism (PHPT) as a hypercalcemic crisis should give rise to the consideration of a differential diagnosis between various different clinical processes for variable prognosis and the consideration of an underlying thyroid pathology.

Cystic parathyroid adenoma is one of its most infrequent causes in the group of glandular cystic neoplasms in the cervix.

The diagnosis of its functional character, supported by the determination of calcemia, blood and intracystic immunoreactive parathormone (PTH<sub>i</sub>), and the interpretation correlated with imaging studies, may contribute to its suspected diagnosis.

Its treatment of choice is surgery by means of selective parathyroidectomy with complete cystic inclusion, and extended to the thyroid depending on their degree of involvement, although this technique may experience modifications depending on the level of confidence in preoperative diagnosis.

**Key words:** *hypercalcemia, parathyroid neoplasia, cyst, hyperparathyroidism.*

## Introduction

Hypercalcemia may be the first manifestation of primary hyperparathyroidism (PHPT), but its expression as a parathyroid crisis is a metabolic emergency which occurs infrequently. Effective medical action is vital to reduce the high risk of mortality associated with it.

A solitary adenoma is usually the most common cause of PHPT<sup>1</sup>, but its presentation in the form of a hypercalcemic crisis requires the consideration of other diagnostic possibilities of disparate prognostic severity, especially if carcinoma is considered.

The concomitance of thyroid pathology with operational repercussions should motivate the carrying out of a preoperative study which clarifies the surgical indication, since the information provided by the imaging tests may distort the importance of this pathology in the absence of specific semiology<sup>2</sup>.

We present a patient with acute PHPT secondary to a cystic parathyroid adenoma concomitant with hyperparathyroidism due to Graves-Basedow disease and a difficult diagnostic interpretation. We report a practical review of the clinical picture which may contribute to its diagnosis and surgical resolution.

## Clinical case

A woman of 57 years of age with a history of hysterectomy due to myoma and in treatment for depression with paroxetine which was evaluated due to a clinical picture of nausea, vomiting, asthenia, loss of 5 kg of weight, polyuria and polydipsia over a number of weeks; detected in the examination were dry mouth and a painless nodule in the lower right cervix, which became mobile with swallowing, without palpable cervical adenopathy or other semiological findings of interest

The analytical study showed calcemia of 14.6 mg/dl (N=8.4-10.2) with corrected calcium of 15.9 mg/dl (N=8.4-10.2), phosphatemia of 2.6 mg/dl (N=2.4-4.7), total proteins of 5.7 g/dl (N=6.4-8.3), albuminemia of 2.6 g/dl (=3.5-5), TSH <  $\mu$ UI/ml (N=0.49-4.67) and  $T_{4L}$  of 3g/dl (N=0.7-1.59).

The patient was initially admitted with a diagnosis of serious hypercalcemia, primary hyperparathyroidism and suspicion of a right thyroid nodule having calciuria of 912 mg (N=100-300) and phosphaturia of 704 mg (N=600-950) for a diuresis of 4,000 ml in 24 hours. Clinical and analytical stability was achieved by means of saline serotherapy at 0.9%, bisphosphonates, furosemide and metimazol. The study was completed in outpatients with PTHi of 1,205.8 pg/ml (N=5-65), thyroid negative anti-peroxidase and anti-TSI receptor antibodies of 1.5 U/L (N=0-0.7)

A thyroid ultrasound showed only one cystic nodule of 3 centimetres in the right inferior pole with PAAF of a clear yellowish liquid containing few inflammatory and no epithelial cells, which was reported to be compatible with the contents of a simple cyst.

A gammagraphy with <sup>99m</sup>Tc-sestamibi (Figure 1A) showed a concentration of pathological captu-

re localised in the upper mediastinum, lateral to the lower pole of the right thyroid, suggestive of ectopic parathyroid adenoma.

With a view to planning for surgery a computerised tomography (CT) was made of the cervix with contrast (Figure 1B) which showed a nodule of 3.6 cm, with mural tumour of a probable parathyroid nature which slightly rectified the lateral right contour of the trachea; and the presence of small jugulodigastric hypocaptive adenopathies.

An en bloc surgical resection was carried out on the patient, which included the right hemithyroidectomy, parathyroidectomy, partial thymectomy with the inclusion of the right paratracheal tissue and lymphadenectomy of the central compartment. The intraoperative PTHi blood determinations were 762.3 pg/ml, 129.4 pg/ml, 110.8 pg/ml and 87.9 pg/ml respectively.

There were no postoperative complications, and the histopathological study was reported as cystic parathyroid adenoma (Figure 2), with no evidence of malignancy in the thymic tissue or in the various isolated adenopathies, and nodular hypoplasia on the right hemithyroid.

During the subsequent follow up the patient took metimazol in reducing doses and had good phospho-calcium metabolism control.

## Discussion

The most common etiology of PHPT is the single adenoma, whose usual form of presentation is hypercalcemia in a postmenopausal patient of between 50 and 60 years of age<sup>1</sup>, and which exceptionally reaches the clinical range of a parathyroid crisis.

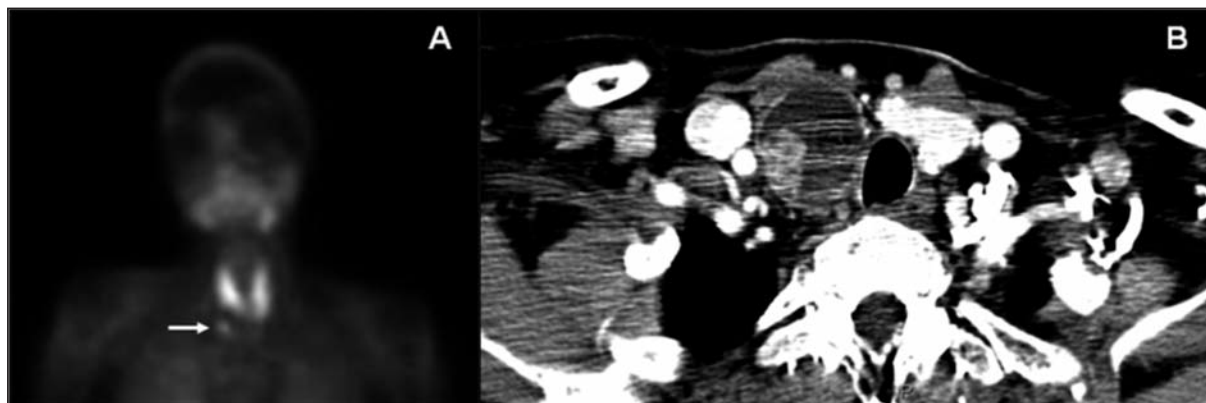
Cystic parathyroid tumours represent 0.6% of thyroid and parathyroid lesions. Their relationship with cystic cervical tumour is lower than 5%<sup>3,4</sup>, and the fact that less than 10% of parathyroid cysts present with hyperparathyroidism make their clinical affiliation difficult<sup>5</sup>.

However, a cystic tumour associated with a hyperparathyroid crisis should point towards a differential diagnosis centred on the different processes which may affect these types of glands. Clinically, various criteria have been proposed to suggest malignancy<sup>6</sup>, such as the presence of a palpable tumour greater than 3 cm, calcemia above 14 mg/dl or semiology of serious hyperparathyroidism.

In addition, there is a close association of around 40% between PHPT and some types of essentially benign concomitant thyroid pathology<sup>7</sup>, with surgical implications which mean that they ought to be considered preoperatively with the aim of planning the surgery strategy. In our patient the formation of the cyst was interpreted as being related to the thyroid, since there was concomitant primary hyperthyroidism independently of suspicious adenoma tissue in the parathyroid.

The parathyroid glands show a great variability in terms of number, size, shape and location, but the diagnosis by imaging of a cystic lesion in the

Figure 1. Composition of radiological sequences showing evidence of parathyroid lesion: gammagraphy with  $^{99m}\text{Tc}$ -sestamibi showing a single pathological hypercapture focus suggestive of ectopic adenoma in upper mediastinum (A). Axial CT section with well-delineated hypodense nodule in the right lobe of the thyroid which contains a hypercapture nodule in its lateral wall and results in slight tracheal compression (B)



vicinity of a structure radiologically compatible with parathyroid tissue in the caudal region of the neck, and concomitant with acute PHPT, means that its relationship with these glands should be discounted, although the possibility of cystic formations or functional alterations in the thyroid may be contemplated. Our patient is a manifest example of this semiological interrelationship.

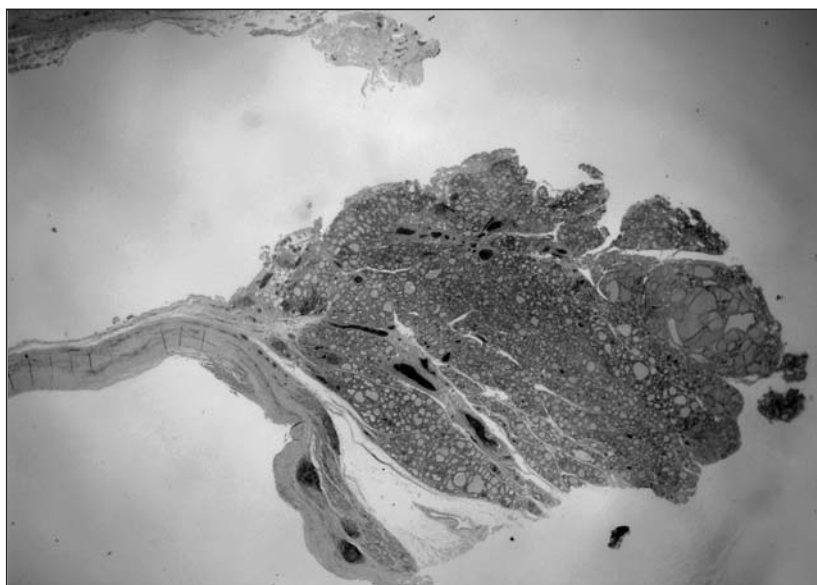
We should also consider that the parathyroid microcysts are frequently found in healthy glands due to the infiltration of fat over time, but that macrocysts are exceptional, and most frequently affect the lower parathyroid, although their clinical repercussions differ according to whether the cyst is functional or non-functional<sup>8,9</sup>.

The former essentially affect men, with hypercalcemia above 13 mg/dl as an indicator of PHPT, and without precise anatomical location, which explains a variable expression: from the absence of symptoms to dyspnoea, dysphonia or dysphagia, according to the structure compromised by its growth<sup>9</sup>. The presence of intracystic haemorrhage could influence an erroneous diagnosis of malignancy.

On the other hand, the non-functional macrocysts predominantly found in women, comprise 90% of the total and lack metabolic activity.

This classification emphasises the importance of our contribution dealing as it does with a woman with lower glandular affection of a functional character.

Figure 2. Histological section of a cystic formation of a fibrous capsule covered with parietal cells, in whose wall can be identified parathyroid tissue with adenomal characteristics and doubtful images of capsular pseudoinvasion. Stained with H-E. 4 x



Its genesis was not clear<sup>10</sup>, although it was thought that it could be derived from the growth and secretion of colloid from primordial cells persisting in the third and fourth branchial cleft, or in the fusion of microcysts in healthy glands. In both theories the cystic tumours would probably not be functional, and their clinical translation would be anecdotal, since this happens with a rise in intracystic PTH without hypercalcemia.

On the other hand, if the cystic tumour derives from the degeneration of an existing parathyroid adenoma, as is possible in this case, the presence of hypercalcemia will define its functional character by the raised levels of blood and intracystic PTH. The presence of haemorrhagic intracystic

foci may also support its adenomal origin. Some authors associate cystic haemorrhage with the appearance of hypercalcemic crisis<sup>11</sup>.

These characteristics should serve to support the clinical diagnosis due to the current limitations in imaging studies which do not usually provide practical details beyond their cystic nature if there is no well-founded clinical suspicion, resulting frequently in their erroneous association with the thyroid gland, as was the case with our patient. In these cases what may be of great help is a fine needle puncture, to obtain a clear liquid with a high concentration of PTH.

This test could have avoided the carrying out of two image tests which facilitate neither diagnosis nor surgical planning, since while they point towards a thyroid pathology, they do not clarify the origin of the cystic tumour, nor discount the possibility of malignancy.

Hence, we consider that any patient with hypercalcemia and high blood PTHi in whom ultrasound of the thyroid shows a cystic lesion should be subject to a PAAF of the lesion in order to determine PTH, and a gammagraphy <sup>99m</sup>Tc-MIBI due to the high sensitivity and specificity of this<sup>12</sup> for a solitary parathyroid adenoma compared with other imaging techniques, with the aim of evaluating a selective cervical approach, although some authors emphasise the value of ultrasound in the hands of expert radiologists for those suspicious cases of cystic adenoma, because of the scarceness of parathyroid tissue in the periphery and a rapid sweep of the scanner may contribute to false negatives<sup>4,13</sup> in these cases.

In our patient the gammagraphy was capable of identifying the adenoma, but could not relate it to the adjacent cystic formation which was considered to be dependent on the thyroid gland.

The other imaging studies should be limited to very specific cases, due to their limited contribution.

Proper preoperative information could contribute to reducing the aggressiveness of surgery, based on the possibility of a hypercalcemic crisis of a malign nature. In our patient, a more reliable diagnosis of benignity would have limited the resection of the parathyroid cyst and the adjacent thyroid tissue, the cyst being partially included in it.

The diagnostic complexity of this pathology would justify a meticulous surgical examination of the other glands<sup>11</sup> in order to discount a multiglandular disease in the form of individualised coexistences of cysts and adenoma, of polyglandular cystic affection or of concomitant hyperplastic disease, although the determination of intraoperative PTH could point us towards the persistence or resolution of the process with greater reliability once the suspicious tissue has been extirpated<sup>14</sup>, reducing surgery time and the risk of morbidity associated with unnecessary explorations.

In conclusion, the scarcity of cases documented in the literature may make difficult the suspected preoperative diagnosis of a benign functional cystic parathyroid tumour, whose confirmation

requires compliance with clinical and biochemical criteria of hyperparathyroidism, identification of parathyroid tissue in the cystic wall in the absence of histological signs of malignancy, morphological or functional demonstration of the normal character of the remaining glands, and the regularization of postoperative levels of calcemia.

**Declaration of interest:** The authors declare the absence of any conflict of interest in this publication.

## Bibliography

1. Fraser WD. Hyperparathyroidism. *Lancet* 2009;374:145-58.
2. Braccini F, Epron JP, Roux C, Gabert K, Richard-Vitton T, Korchia D, et al. Le kyste parathyroïdien essentiel: une affection trompeuse. *Rev Laryngol Otol Rhinol (Bord)* 2000;121:165-8.
3. Martí J, Martín Arregi FJ, Mutio L, Alonso A. Quiste paratiroideo. A propósito de un caso. *Acta Otorrinolaringol Esp* 2002;53:302-4.
4. Wirowski D, Wicke C, Böhner H, Lammers BJ, Pohl P, Schwarz K, et al. Presentation of 6 cases with parathyroid cysts and discussion of the literature. *Exp Clin Endocrinol Diabetes* 2008;116:501-6.
5. Serra Soler G, García Fernández H, Quevedo Juanals J, Argüelles Jiménez I, Carrillo García P. Crisis paratiroidea por adenoma quístico de paratiroides. *Endocrinol Nutr* 2011;58:148-50.
6. Chang YJ, Mittal V, Remine S, Manyam H, Sabir M, Richardson T, et al. Correlation between clinical and histological findings in parathyroid tumors suspicious for carcinoma. *Am Surg* 2006;72:419-26.
7. Laing VO, Frame B, Block MA. Associated primary hyperparathyroidism and thyroid lesions. Surgical considerations. *Arch Surg* 1969;98:709-12.
8. Gurbuz AT, Peetz ME. Giant mediastinal parathyroid cyst: an unusual cause of hypercalcemic crisis – case report and review of the literature. *Surgery* 1996;120:795-800.
9. Khan A, Khan Y, Raza S, Akbar G, Khan M, Diwan N, et al. Functional parathyroid cyst: a rare cause of malignant hypercalcemia with primary hyperparathyroidism – a case report and review of the literature. *Case Report Med* 2012;2012:851941, 5 pages.
10. Fortson JK, Patel VG, Henderson VJ. Parathyroid cysts: a case report and review of the literature. *Laryngoscope* 2001;111:1726-8.
11. Manouras A, Toutouzas KG, Markogiannakis H, Lagoudianakis E, Papadima A, Antonakis PT, et al. Intracystic hemorrhage in a mediastinal cystic adenoma causing parathyrotoxic crisis. *Head Neck* 2008;30:127-31.
12. Richards MK, Slavin ER, Tamarkin SW, McHenry CR. Technetium-99m sestamibi imaging: Are the results dependent on the review

- wer? J Surg Res 2012;177:97-101.
13. Tublin ME, Pryma DA, Yim JH, Ogilvie JB, Mountz J, Bencherif B, et al. Localization of parathyroid adenomas by sonography and technetium Tc 99m sestamibi single-photon emission computed tomography before minimally invasive parathyroidectomy: are both studies really needed? J Ultrasound Med 2009;28:183-90.
  14. Mazeh H, Sippel RS, Chen H. Three large, functioning cystic parathyroid adenomas. Endocr Prat 2012;18:14-6.